

Stretching Semiflexible Polymer Chains: Evidence for the Importance of Excluded Volume Effects from Monte Carlo Simulation

Hsiao-Ping Hsu* and Kurt Binder

Institut für Physik, Johannes Gutenberg-Universität Mainz, Staudinger Weg 7, D-55099 Mainz, Germany

(Dated: May 24, 2022)

Semiflexible macromolecules in dilute solution under very good solvent conditions are modeled by self-avoiding walks on the simple cubic lattice ($d = 3$ dimensions) and square lattice ($d = 2$ dimensions), varying chain stiffness by an energy penalty ϵ_b for chain bending. In the absence of excluded volume interactions, the persistence length ℓ_p of the polymers would then simply be $\ell_p = \ell_b(2d-2)^{-1}q_b^{-1}$ with $q_b = \exp(-\epsilon_b/k_B T)$, the bond length ℓ_b being the lattice spacing, and $k_B T$ is the thermal energy. Using Monte Carlo simulations applying the pruned-enriched Rosenbluth method (PERM), both q_b and the chain length N are varied over a wide range ($0.005 \leq q_b \leq 1$, $N \leq 50000$), and also a stretching force f is applied to one chain end (fixing the other end at the origin). In the absence of this force, in $d = 2$ a single crossover from rod-like behavior (for contour lengths less than ℓ_p) to swollen coils occurs, invalidating the Kratky-Porod model, while in $d = 3$ a double crossover occurs, from rods to Gaussian coils (as implied by the Kratky-Porod model) and then to coils that are swollen due to the excluded volume interaction. If the stretching force is applied, excluded volume interactions matter for the force versus extension relation irrespective of chain stiffness in $d = 2$, while theories based on the Kratky-Porod model are found to work in $d = 3$ for stiff chains in an intermediate regime of chain extensions. While for $q_b \ll 1$ in this model a persistence length can be estimated from the initial decay of bond-orientational correlations, it is argued that this is not possible for more complex wormlike chains (e.g. bottle-brush polymers). Consequences for the proper interpretation of experiments are briefly discussed.

PACS numbers:

I. INTRODUCTION

The response of macromolecules with linear chemical architecture to mechanical forces pulling at their ends has been a longstanding problem in the statistical mechanics of polymers [1–29]. Particular interest in this problem is due to advances in experimental techniques of single molecule measurements, probing the tension-induced stretching of biological macromolecules such as DNA [30], RNA [31], proteins [32] and polysaccharides [33]. But also insight into the structure-property relationships of synthetic polymers, e.g. bottle brushes [34], has been gained by such experiments. However, despite extensive work on these problems, important aspects are still not well understood, even for the relatively simple case of macromolecules in dilute solutions of good solvent quality, disregarding the interesting interplay of chain stretching and collapse that occurs in poor solvents [26, 35–38], and also the interplay of chain stretching and adsorption on substrates [39–42].

An important aspect of these problems is local chain stiffness. Traditionally, chain stiffness is characterized by “the” persistence length [1, 9] but evidence has been presented [43–45] that the traditional definitions are not useful under good solvent conditions, where excluded volume interactions create long range correlations with respect to the conformational properties of a macromolecule [6, 46]. For stretched flexible polymers under a force f the stan-

dard theory uses the concept of “Pincus blobs” [5], of size $\xi_P = k_B T/f$, $k_B T$ being the thermal energy, predicting a crossover from a Hookean regime, where the extension $\langle X \rangle$ for a force (applied in x -direction) scales as $\langle X \rangle = \langle R^2 \rangle (f/dk_B T)$ in d dimensions, to a nonlinear power law $\langle X \rangle \propto f^{1/\nu-1}$ (ν being the Flory exponent, $\nu \approx 3/5$ in $d = 3$ dimensions). In contrast, for stretched semiflexible polymers excluded volume is widely neglected in the literature [12, 13, 18–20] and using the Kratky-Porod model (K-P model) [47, 48] simple analytic relations between force f and relative extension $\langle X \rangle/L$, L being the contour length of the polymer, are derived [12, 24]. We recall that $L = N_b \ell_b$ where N_b is the number of effective bonds of length ℓ_b connecting the effective monomeric units of the macromolecule, and if excluded volume interactions were absent, we would have, for $N_b \rightarrow \infty$ in the absence of the force f , the end-to-end distance of the polymer chains as (the index “0” refers to $f = 0$)

$$\langle R^2 \rangle_0 = \ell_k L = 2\ell_p L = \ell_k^2 n, \quad (1)$$

$\ell_k = 2\ell_p$ being the length of a Kuhn segment, $n = N_b \ell_b / \ell_k$ being the number of such Kuhn segments forming the equivalent freely jointed chain [1, 6]. However, neither ℓ_k nor ℓ_p can be defined straightforwardly in the presence of excluded volume forces [43–46, 49].

With recent large scale computer simulations, we have studied the combined effects of local “intrinsic” chain stiffness and excluded volume interactions on the conformational properties of polymers in the absence of stretching forces, both for $d = 3$ [43, 44] and $d = 2$ [45] dimensions. The present study extends this work, giving a

*Electronic address: hsu@uni-mainz.de

detailed study of force-extension relations for both $d = 2$ and $d = 3$, complementing our results also by investigating fluctuations $\langle X^2 \rangle - \langle X \rangle^2$, $\langle R_{\perp}^2 \rangle$ of the chain linear dimensions in the direction of the force and perpendicular to it. Whenever possible, a comparison with theoretical predictions will be given. Since our study is based on modelling polymers as self-avoiding walks on square and simple cubic lattices, the main focus of our work is on the regime of low and intermediate forces (for very high forces, a more realistic description of the local structure and energetics of a polymer chains, such as bond length, bond angle and torsional potentials, becomes important [23]).

The outline of our paper is as follows: in Sec. II, we summarize the state of the art, discussing in particular the theoretical results we want to compare to. Sec. III briefly describes our model and the simulation technique, while Sec. IV reviews the properties of chains in the absence of stretching forces. Sec. V describes the effects of stretching forces on conformational properties in $d = 2$ and Sec. VI in $d = 3$ dimensions. Finally Sec. VII gives a summary and an outlook on experimental work, as well as on the related but more complicated problem of the ‘‘electrostatic persistence length’’ in polyelectrolytes (see [50] for a review and further references).

II. THEORETICAL BACKGROUND

A. Force-Extension Curves for Flexible Chains

Suppose we fix one end of an isolated polymer chain at the origin and apply a force $\vec{f} = (f, 0, 0)$ acting along the x-axis to the other chain end. This means, we add to the Hamiltonian of the chain a potential

$$U = -fX \quad (2)$$

where X is the x-component of the end-to-end vector \vec{R} of the chain. Noting that $\vec{R} = \sum_{i=1}^{N_b} \vec{a}_i$, where $\vec{a}_i = \vec{r}_{i+1} - \vec{r}_i$ is the bond vector connecting monomers, at sites \vec{r}_i and \vec{r}_{i+1} , with $|\vec{a}_i| = \ell_b$ the bond length which we assume as a constant, X can be rewritten as

$$X = \ell_b \sum_{i=1}^{N_b} \cos \vartheta_i, \quad (3)$$

where ϑ_i is the angle between \vec{a}_i and the x-axis. For a model of freely jointed chains (FJC), a straightforward calculation of the partition function of the chain yields the force versus extension curve in terms of the Langevin function [3, 4, 9, 51] (in $d = 3$ dimensions)

$$\langle X \rangle = \ell_b N_b \mathcal{L}(f \ell_b / k_B T) \quad (\text{FJC}), \quad (4)$$

$$\mathcal{L}(\zeta) = \coth(\zeta) - 1/\zeta, \quad \zeta \equiv f \ell_b / k_B T. \quad (5)$$

Note that $\mathcal{L}(\zeta \ll 1) \approx \zeta/3$ and hence one finds for small forces that

$$\begin{aligned} \langle X \rangle &\approx \frac{1}{3} \ell_b^2 N_b f / k_B T = \langle R^2 \rangle_0 f / (3k_B T), \\ \langle X \rangle / L &\approx f \ell_b / (3k_B T) \quad (\text{FJC}), \end{aligned} \quad (6)$$

where $\langle R^2 \rangle_0 = \ell_b^2 N_b$ for a freely jointed chain. Eq. (6) would apply for Gaussian chains in the continuum for arbitrary large extensions, while for the freely jointed chain Eqs. (4), (5) describe a saturation behavior for large f , when $\langle X \rangle$ approaches the contour length $L = N_b \ell_b$, as

$$\langle X \rangle / L \approx 1 - k_B T / f \ell_b \quad (\text{FJC}). \quad (7)$$

Of course, excluded volume interactions significantly modify the behavior described by Eqs. (4)-(6). Already in the absence of the force, Eq. (1) is replaced by

$$\langle R^2 \rangle_0 = C \ell_b^2 N_b^{2\nu}, \quad N_b \rightarrow \infty \quad (\text{SAW}), \quad (8)$$

where C is a (non-universal, i.e. model - or system-dependent) constant of order unity, and the exponent $\nu \approx 0.588$ in $d = 3$ dimensions [52, 53] while $\nu = 3/4$ in $d = 2$ dimensions [6, 9, 53] {Polymer chains behave like self-avoiding walks (SAWs)}. Treating the potential, Eq. (2), as a small perturbation in linear response one can generally show that

$$\langle X \rangle = \langle R^2 \rangle_0 f / (dk_B T) \quad \text{for small } f \quad (9)$$

and hence the relative extension becomes in this regime

$$\langle X \rangle / L = C (L / \ell_b)^{2\nu-1} (f \ell_b) / (dk_B T) \quad (\text{SAW}). \quad (10)$$

Comparing to Eq. (6) we note that the relative extension is enhanced by a factor $C (L / \ell_b)^{2\nu-1}$ in comparison with the result for the freely jointed chain.

While for the freely jointed chain the linear behavior, Eq. (6), smoothly crosses over to the saturation behavior $\langle X \rangle / L \rightarrow 1$, Eq. (7), for the swollen coil there occurs an intermediate regime with a nonlinear relation between extension and force. This regime was first discussed by Pincus [5] in terms of the scaling ansatz

$$\langle X \rangle = \langle R^2 \rangle_0^{1/2} F(\langle R^2 \rangle_0^{1/2} / \xi_P) \quad (\text{SAW}), \quad (11)$$

where ξ_P is the radius of a ‘‘tensile blob’’ (also called now ‘‘Pincus blob’’),

$$\xi_P = k_B T / f, \quad (12)$$

and F is a scaling function. Of course, this description makes only sense if

$$\ell_b \ll \xi_P \ll \langle R^2 \rangle_0^{1/2}, \quad (13)$$

since the scaling law for a blob ($\xi_P \approx \ell_b g^\nu$ with g monomers per blob) breaks down when g is no longer very large; then a gradual crossover to the behavior of

a strongly stretched freely jointed chain must occur (excluded volume then becomes irrelevant). For ξ_P of order $\langle R^2 \rangle_0^{1/2}$, $F(\eta)$ behaves as $(\eta \equiv \langle R^2 \rangle_0^{1/2}/\xi_P)$

$$F(\eta) = \eta/d \quad (14)$$

so that Eq. (11) reduces to the linear response results, Eq. (9). In the regime where Eq. (13) holds, the conformation of the chain is a stretched string of N_b/g blobs, i.e. in order to obtain $\langle X \rangle \propto L$ one must require that $F(\eta) \propto \eta^{1/\nu-1}$ and hence

$$\langle X \rangle \propto \xi_P N_b/g \propto (k_B T/f\ell_b)^{1-1/\nu} L \text{ (SAW)}, \quad (15)$$

and hence one finds that in this regime the relative extension varies as

$$\langle X \rangle/L \propto (f\ell_b/k_B T)^{1/\nu-1} \text{ (SAW)}. \quad (16)$$

In a biopolymer context, this old result due to Pincus [5] was recently “rediscovered” by Lam [54]. This scaling behavior can be made somewhat more explicit using the scaling description of the distribution $P_{N_b}(X)$ in which (in the absence of a stretching force f) a displacement X between two end monomers occurs [10]

$$\langle X \rangle = k_B T \partial \ln Z(f)/\partial f \text{ (SAW)}, \quad (17)$$

where the partition function $Z(f)$ is (Z_0 is a normalization constant out of interest here)

$$Z(f) = Z_0 \int d^d \vec{R} P_{N_b}(X) \exp(fX/k_B T). \quad (18)$$

Using the ansatz [53]

$$P_{N_b}(X) \propto h(y) \propto y^\phi \exp[-Dy^{1/(1-\nu)}], \quad (19)$$

where $y \equiv X/\langle R^2 \rangle_0^{1/2}$, $\phi = (1 - \gamma + \nu d - d/2)/(1 - \nu)$, γ is a standard critical exponent [6] and D is a constant, Eqs. (17), (18) can be worked out numerically.

Wittkop et al. [10] derived Eq. (16) without explicit recourse to a blob picture. Wittkop et al. [10] tried also to provide Monte Carlo evidence for Eq. (16), both in $d = 2$ and $d = 3$, but they had to restrict their study to very short chains ($20 \leq N_b \leq 100$). Morrison et al. [25] argued that chain lengths of at least $N_b = 10^3$ are necessary to provide clear simulation evidence for the Pincus tensile blob regime (described by Eqs. (13), (16)). In fact, using $N_b = 6000$ Pierleoni et al. [14] succeeded to obtain evidence in favor of the Pincus theory [5] for the chain structure factor under stretch. However, we are not aware of systematic tests of Eq. (16) for very large N_b , as shall be presented here.

A very interesting issue are also the longitudinal and transverse fluctuations, in the extensions of stretched chains. For freely jointed chains Titantah et al. [16] derived

$$\langle X^2 \rangle - \langle X \rangle^2 = N_b \ell_b^2 [1 - 2\mathcal{L}(\zeta)/\zeta - \mathcal{L}^2(\zeta)] \text{ (FJC)} \quad (20)$$

which for large $\zeta = f\ell_b/k_B T$ reduces to

$$\langle X^2 \rangle - \langle X \rangle^2 \approx N_b \ell_b^2 \zeta^{-2} = (k_B T/f\ell_b)^2 N_b \ell_b^2 \text{ (FJC)}. \quad (21)$$

The transverse fluctuations becomes

$$\begin{aligned} \langle R_\perp^2 \rangle &= \langle Y^2 \rangle + \langle Z^2 \rangle \\ &= 2N_b \ell_b^2 \mathcal{L}(\zeta)/\zeta \approx 2N_b \ell_b^2 (k_B T/f\ell_b) \text{ (FJC)} \end{aligned} \quad (22)$$

where the last expression again refers to $f \rightarrow \infty$. Of course, Eq. (22) differs substantially from a continuum Gaussian model of a chain (there the transverse linear dimensions are not affected by the pulling force at all).

In the case where excluded volume is taken into account, one obtains using again an approach based on Eqs. (17)-(19) the approximate expressions [16]

$$(\langle X^2 \rangle - \langle X \rangle^2)/\langle R^2 \rangle_0 = \frac{s_3}{s_1} - \left(\frac{c_2}{s_1}\right)^2 + \zeta^{-2} \text{ (SAW)}, \quad (23)$$

$$\langle R_\perp^2 \rangle/\langle R^2 \rangle_0 = \zeta^{-2} [\zeta c_2/s_1 - 1] \text{ (SAW)}, \quad (24)$$

where the functions $s_i(\zeta)$ and $c_i(\zeta)$ are defined as

$$s_i(\zeta) = \int_0^\infty dy \sinh(\zeta y) y^{i+\phi} \exp[-Dy^{1/(1-\nu)}], \quad i = 1, 3, \quad (25)$$

and

$$c_i(\zeta) = \int_0^\infty dy \cosh(\zeta y) y^{i+\phi} \exp[-Dy^{1/(1-\nu)}], \quad i = 1, 2. \quad (26)$$

Alternative approximate expressions were derived by Morrison et al. [25] using the self-consistent variational method due to Edwards and Singh [55].

B. Semiflexible chains in the absence of stretching forces: Chain linear dimensions and bond vector orientational correlations

Following Winkler [20, 56] we first consider a chain with fixed bond length ℓ_b but successive bonds are correlated with respect to their relative orientations,

$$\langle \vec{a}_i^2 \rangle = \ell_b^2, \quad \langle \vec{a}_i \cdot \vec{a}_{i+1} \rangle = \ell_b^2 t, \quad t \equiv \langle \cos \theta \rangle, \quad (27)$$

θ being the angle between the orientation of two successive bond vectors. For this model, in the absence of excluded volume effects, the end-to-end distance is well-known [1, 56]

$$\langle R^2 \rangle_0 = N_b \ell_b^2 \left(\frac{1+t}{1-t} + \frac{2t}{N_b} \frac{t^{N_b} - 1}{(t-1)^2} \right) \quad (28)$$

In the limit $N_b \rightarrow \infty$ the correlation function of bond vectors decays exponentially as a function of their chemical distance s ,

$$\langle \vec{a}_i \cdot \vec{a}_{i+s} \rangle = \ell_b^2 \langle \cos \theta(s) \rangle = \ell_b^2 \langle \cos \theta \rangle^s = \ell_b^2 \exp(-\ell_b s/\ell_p), \quad (29)$$

where we have introduced the notion of the persistence length ℓ_p [9, 51] which becomes in this case

$$\ell_b/\ell_p = -\ln(\langle \cos \theta \rangle). \quad (30)$$

In the case of semiflexible chains one has $\langle \cos \theta \rangle \approx 1 - \langle \theta^2 \rangle/2$, since $\langle \theta^2 \rangle$ then is small, and hence one finds (for $N_b \rightarrow \infty$) [51]

$$\ell_p \approx 2\ell_b/\langle \theta^2 \rangle, \quad \langle R^2 \rangle_0 \approx 4N_b\ell_b^2/\langle \theta^2 \rangle = 2\ell_p\ell_bN_b, \quad (31)$$

so in this limit the Kuhn length ℓ_k {Eq. (1)} becomes $\ell_k = 2\ell_p$, as was anticipated.

When one considers now the limit $\ell_b \rightarrow 0$, $N_b \rightarrow \infty$, keeping $L = \ell_bN_b$ as well as ℓ_p finite, one obtains from Eq. (28) [56]

$$\langle R^2 \rangle_0 = 2\ell_pL\left\{1 - \frac{\ell_p}{L}[1 - \exp(-L/\ell_p)]\right\}, \quad (32)$$

which is nothing but the result that one could have derived directly from the Kratky-Porod model [47, 48] for wormlike chains,

$$\mathcal{H} = \frac{\kappa}{2} \int_0^L \left(\frac{\partial^2 \vec{r}}{\partial s^2} \right)^2 ds, \quad (33)$$

where the polymer chain is described by the contour $\vec{r}(s)$ in continuous space. The bending stiffness κ is related to the persistence length ℓ_p as

$$\kappa = \ell_p k_B T, \quad d = 3, \quad \text{or} \quad \kappa = \frac{\ell_p}{2} k_B T, \quad d = 2. \quad (34)$$

We note in this context the connection to the lattice models that will be studied in the present work, where we study self-avoiding walks on square ($d = 2$) and simple cubic ($d = 3$) lattices, using a ‘‘penalty energy’’ ϵ_b if the chain makes a bend (by a 90° angle). Relaxing the excluded volume constraint by considering a ‘‘non-reversal random walk’’ [57], where only immediate reversals of a simple random walk model would be forbidden, we immediately conclude that

$$\langle \cos \theta \rangle = 1/[1 + (2d - 2)q_b], \quad q_b = \exp(-\epsilon_b/k_B T), \quad (35)$$

and hence one would obtain for $q_b \rightarrow 0$ from Eq. (31) that

$$\ell_p/\ell_b = 1/(2q_b) \quad d = 2, \quad \text{or} \quad \ell_p/\ell_b = 1/(4q_b) \quad d = 3. \quad (36)$$

At this point, it is interesting to recall that the present lattice model can be described by the Hamiltonian $\mathcal{H} = \epsilon_b \sum_i (1 - \vec{a}_i \cdot \vec{a}_j/\ell_b^2) = \epsilon \sum_i (1 - \cos \theta_i)$, plus excluded volume interaction, i.e. it is a discretized version of the Kratky-Porod model plus excluded volume, with angles θ_i restricted to $\theta_i = 0$ and $\theta_i = \pm 90^\circ$, respectively. For a corresponding continuum model for large ϵ small angles would dominate, however: putting $1 - \cos \theta_i \approx \theta_i^2/2$ the

corresponding Hamiltonian would be $\mathcal{H} = (\epsilon_b/2) \sum_i \theta_i^2$ so one would conclude that κ (and hence ℓ_p) are simply proportional to ϵ_b . Eqs. (35), (36) rather imply $\ell_p \propto \exp(\epsilon/k_B T)$; this effect is due to the fact that only large nonzero angles $\pm 90^\circ$ are permitted.

Eq. (32) describes the crossover from the behavior of a rigid rod for $L < \ell_p$, where $\langle R^2 \rangle_0 = L^2$, to Gaussian chains for $L \gg \ell_p$, where Eq. (1) holds, $\langle R^2 \rangle_0 = 2\ell_pL$. However, neither the exponential decay of the correlation function of bond vectors {Eq. (29)} nor the Gaussian behavior implied by Eq. (32) remain valid when excluded volume effects are considered.

On a qualitative level, insight into the effects of excluded volume on semiflexible chains can be gotten by Flory-type free energy minimization arguments [6, 9, 58, 59]. Consider a model where rods of length ℓ_k and diameter D are jointed together, such that the contour length $L = N_b\ell_b = n\ell_k$. Apart from prefactors of order unity, the second virial coefficient then can be estimated as (in $d = 3$ dimensions)

$$v_2 = \ell_k^2 D. \quad (37)$$

The free energy of a chain now contains two terms, the elastic energy and the energy due to the excluded volume interactions embodied in Eq. (37). The elastic energy is taken as that of a free Gaussian chain, i.e. $F_{el} \approx R^2/(\ell_kL)$. The repulsive interactions are treated in mean field approximation, i.e. proportional to the square of the density n/R^3 and the volume R^3 . Thus

$$\Delta F/k_B T \approx R^2/(\ell_kL) + v_2 R^3[(L/\ell_k)/R^3]^2 \quad (38)$$

Minimizing ΔF with respect to R , we find for $L \rightarrow \infty$ the standard Flory result

$$R \approx (v_2/\ell_k)^{1/5} L^{3/5} = (\ell_k D)^{1/5} (N_b \ell_b)^{3/5}. \quad (39)$$

However, for finite L (or finite N_b , respectively), Eq. (39) applies only when the chain length N_b exceeds the crossover length N_b^* or when R exceeds the associate radius R^* ,

$$N_b > N_b^*, \quad N_b^* = \ell_k^3/(\ell_b D^2), \quad R^* = \ell_k^2/D. \quad (40)$$

If $N_b < N_b^*$ the contribution of the second term in Eq. (38) would still be negligible for $R^2 \approx \ell_kL$, where $\Delta F/k_B T$ is of order unity, and hence for $N_b < N_b^*$ the first term in Eq. (38) dominates, and hence the chain behaves like a Gaussian coil. However, this Gaussian regime only exists if $N_b^* \gg N_b^{\text{rod}} = \ell_k/\ell_b$, the number of monomers per Kuhn length. For $N_b < N_b^{\text{rod}}$, the chain resembles a rigid rod. Thus we predict (in $d = 3$) two subsequent crossovers:

$$R \approx L, \quad N_b < N_b^{\text{rod}} = \ell_k/\ell_b \text{ (rod-like chain)}, \quad (41)$$

$$R \approx (\ell_kL)^{1/2}, \quad N_b^{\text{rod}} < N_b < N_b^* \text{ (Gaussian coil)}, \quad (42)$$

$$R \approx (\ell_kD)^{1/5} L^{3/5}, \quad N_b > N_b^* (R > R^*) \text{ (SAW)}. \quad (43)$$

Of course, the intermediate Gaussian regime of Eq. (42) only exists if $N_b^* \gg N_b^{\text{rod}}$, or alternatively

$$\ell_k \gg D. \quad (44)$$

E.g., in the case of bottle brush polymers with flexible backbone chains and flexible side chains under good solvent conditions evidence has been presented for the fact that the stiffness of these wormlike chains is only due to their thickness [43, 44], and hence ℓ_k and ℓ_p are of the same order as D (disregarding the difficulty to define either ℓ_k or ℓ_p in this case properly) and thus the intermediate Gaussian regime does not occur. On the other hand, for a large number of real semiflexible macromolecules under good solvent conditions the double crossover described by Eqs. (41)-(43) has been clearly observed [60].

On the other hand, the situation is completely different in $d = 2$ dimensions, where Eq. (37) is replaced by

$$v_2 = \ell_k^2 \quad (45)$$

since a rod of length ℓ_k blocks an area of order ℓ_k^2 by occupation from a (differently oriented) second rod. Eq. (38) in $d = 2$ becomes [45]

$$\Delta F/k_B T \approx R^2/(\ell_k L) + v_2 R^2[(L/\ell_k)/R^2]^2. \quad (46)$$

Minimizing again ΔF with respect to R yields now

$$R \approx (v_2/\ell_k)^{1/4} L^{3/4} \approx \ell_k^{1/4} L^{3/4}, \quad d = 2, \quad (47)$$

where now the size $L^* = \ell_b N_b^*$ where Eq. (47) starts to hold is

$$L^* = \ell_k, \quad \text{i.e. } N_b^* = N_b^{\text{rod}}. \quad (48)$$

Thus we note that a direct crossover occurs from rods to swollen coils (exhibiting statistical properties of two-dimensional self-avoiding walks), and no regime with intermediate Gaussian behavior occurs.

An important consequence of the excluded volume interaction is that they cause a much slower asymptotic decay of orientational correlations than described by Eq. (29) occurs. For fully flexible chains one has a power law [46]

$$\langle \vec{a}_i \cdot \vec{a}_{i+s} \rangle \propto s^{-\beta}, \quad \beta = 2(1 - \nu), \quad 1 \ll s \ll N_b. \quad (49)$$

Eq. (49) has been verified by extensive Monte Carlo simulations of self-avoiding walks on simple cubic ($d = 3$) [43, 44] and square ($d = 2$) [45] lattices; we shall recall these results and extend them in Sec. IV below.

For semiflexible chains we expect a crossover from exponential decay {Eq. (29)} to the power law {Eq. (51)} to occur near $s = N_b^*$, i.e. we make the speculative assumption that

$$\langle \vec{a}_i \cdot \vec{a}_{i+s} \rangle \approx \ell_b^2 \exp(-s\ell_b/\ell_p), \quad 1 \ll s \ll N_b^*, \quad (50)$$

$$\langle \vec{a}_i \cdot \vec{a}_{i+s} \rangle \approx \exp(-N_b^* \ell_b/\ell_p) \ell_b^2 \left(\frac{s\ell_b}{L^*}\right)^{-\beta}, \quad N_b^* \ll s \ll N_b. \quad (51)$$

Note that the prefactor of the power law in Eq. (51) was chosen such that for $s = N_b^*$ (where $s\ell_b = L^*$) a smooth crossover to Eq. (50) is possible. In $d = 2$, where $N_b^* = N_b^{\text{rod}}$, and hence $N_b^* \ell_b = \ell_k = 2\ell_p$, we note that the factor $\exp(-N_b^* \ell_b/\ell_p) \approx 0.14$ and using $\beta = 1/2$ in $d = 2$ one finds that

$$\langle \vec{a}_i \cdot \vec{a}_{i+s} \rangle / \ell_b^2 \approx 0.14(2\ell_p/\ell_b)^{1/2} s^{-1/2}, \quad N_b^* \ll s \ll N_b \quad (52)$$

and hence there occurs an increase of the amplitude of the power law with ℓ_p . However, in $d = 3$, where $N_b^*/N_b^{\text{rod}} = (2\ell_p/D)^2$ the factor $\exp(-N_b^* \ell_b/\ell_p) = \exp(-2N_b^*/N_b^{\text{rod}}) = \exp[-8(\ell_p/D)^2]$ for large ℓ_p will dominate and hence lead to a strong decrease of the amplitude of the power law in Eq. (51). Of course, the crossover at N_b^* is not at all sharp but rather spread out over several decades in s , and hence the observability of Eqs. (50), (51) is rather restricted. Note, however, that $\langle \vec{a}_i \cdot \vec{a}_{i+s} \rangle$ always exhibits a single crossover only (for $N_b^* \rightarrow \infty$), near $s = N_b^*$: while the radius exhibits two crossovers in $d = 3$ (at $N_b = N_b^{\text{rod}}$ and at $N_b = N_b^*$), Eq. (50) does not exhibit any change in behavior when $s \approx N_b^{\text{rod}} = 2\ell_p/\ell_b$. Thus we predict that for very stiff and thin chains (for which ℓ_p/D and hence N_b^*/N_b^{rod} are large numbers) one can follow the exponential decay $\exp(-s\ell_b/\ell_p)$ over several decades. In $d = 2$, where $N_b^* = N_b^{\text{rod}}$, this is predicted to be impossible; rather one can follow the exponential decay only from unity to about $1/e$. We shall discuss in Sec. IV a Monte Carlo test of these predictions.

C. Stretching of semiflexible chains

There exists a rich literature [12, 13, 18–20, 24–26, 28] where a force term, Eq. (2), is added to the Kratky-Porod Hamiltonian, Eq. (33), to obtain

$$\mathcal{H} = \frac{\kappa}{2} \int_0^L \left(\frac{\partial^2 \vec{r}(s)}{\partial s^2}\right)^2 ds - f \int_0^L \frac{\partial x(s)}{\partial s} ds. \quad (53)$$

We shall not dwell here on the exact numerical methods by which force versus extension curves can be derived from Eq. (53), but simply quote approximate interpolation formulas [12, 24] (which are known to deviate from the numerically exact solutions at most by a few percent),

$$\frac{f\ell_p}{k_B T} = \frac{\langle X \rangle}{L} + \frac{1}{4(1 - \langle X \rangle/L)^2} - \frac{1}{4}, \quad d = 3 \quad (\text{K-P model}), \quad (54)$$

$$\frac{f\ell_p}{k_B T} = \frac{3\langle X \rangle}{4L} + \frac{1}{8(1 - \langle X \rangle/L)^2} - \frac{1}{8}, \quad d = 2 \quad (\text{K-P model}). \quad (55)$$

At this point, we remind the reader that $\kappa = \ell_p k_B T$ in $d = 3$ while $\kappa = \ell_p k_B T/2$ in $d = 2$ {Eq. (34)}. For small

f , Eqs. (54), (55) are compatible with the relations that one can derive by treating f via linear response, $\langle X \rangle = f \langle X^2 \rangle_0 / k_B T$ and hence $\langle X^2 \rangle_0 = \langle R^2 \rangle_0 / d = 2\ell_p L / d$

$$\frac{f\ell_p}{k_B T} = \frac{d \langle X \rangle}{2L}, \quad d = 2, 3 \text{ (K - P model)}, \quad (56)$$

while for large f we find

$$\langle X \rangle / L \approx 1 - 1 / \sqrt{4f\ell_p / k_B T}, \quad d = 3 \text{ (K - P model)}, \quad (57)$$

or

$$\langle X \rangle / L \approx 1 - 1 / \sqrt{8f\ell_p / k_B T}, \quad d = 2 \text{ (K - P model)}. \quad (58)$$

A further quantity of interest is the ‘‘deflection length’’ [61, 62], i.e. the correlation length of fluctuations along a semiflexible polymer. In the presence of a strong force it is given by [19]

$$\lambda = (f / k_B T \ell_p)^{-1/2}, \quad \text{or } \lambda / \ell_p = (f \ell_p / k_B T)^{-1/2}. \quad (59)$$

When $f\ell_p$ exceeds $k_B T$, λ hence becomes smaller than ℓ_p , and in this limit one expects that excluded volume indeed becomes negligible. However, when λ becomes of the order of the bond length ℓ_b , it is clear that the continuum description in terms of Eq. (53) breaks down, the discreteness of the chain molecule becomes relevant [19, 22, 25], and a crossover to the behavior of a freely jointed polymer occurs, as was described by Eq. (7). Toan and Thirumalai [28] have emphasized that all polymers under sufficiently high stretching forces should show a crossover from a force law of the type of the Kratky-Porod model, $1 - \langle X \rangle / L \propto f^{-1/2}$ {Eqs. (57), (58)}, to the law of the freely jointed model, $1 - \langle X \rangle / L \propto f^{-1}$ {Eq. (7)}, and they argued that the crossover force between both descriptions is obtained by putting $\lambda = \ell_b$, providing evidence for this concept both by an analysis of experimental data and by a study of various models. However, here we are mostly interested in the regime where $\langle X \rangle / L$ is significantly smaller than unity, and excluded volume effects are still relevant.

In particular, for weak forces we can combine Eq. (9) with the proper relations for the linear dimensions of the semiflexible chains, as discussed in Eq. (39) for $d = 3$ and Eq. (47) for $d = 2$, respectively. Thus, Eq. (56) gets replaced by

$$\langle X \rangle / L \propto (f \ell_p / k_B T) (D / \ell_p)^{2/5} (L / \ell_p)^{1/5}, \quad L > L^* = \ell_b N_b^* \quad (60)$$

in $d = 3$, while in $d = 2$ we have

$$\langle X \rangle / L \propto (f \ell_p / k_B T) (L / \ell_p)^{1/2}, \quad L > \ell_p, \quad (61)$$

where factors of order unity have been disregarded throughout. We note that in this regime the relations $\langle X \rangle / L$ versus $f \ell_p / k_B T$ vary much more steeply than predicted by Eq. (56) if L / ℓ_p is very large. Furthermore we note from Eqs. (9)-(16) that the nonlinear Pincus force-extension relation, Eq. (16), sets in when the size of the

Pincus blob is of the same order as the coil size $\sqrt{\langle R^2 \rangle_0}$ (Eq. (39) for $d = 3$, or Eq. (47) for $d = 2$, in the absence of a force), defining a crossover length $\xi_{P,c}$ and associated force f_c ,

$$\begin{aligned} \xi_{P,c} &= \frac{k_B T}{f_c} = (\ell_p D)^{1/5} L^{3/5}, \quad d = 3, \\ &\text{or} \\ \xi_{P,c} &= \ell_p^{1/4} L^{3/4}, \quad d = 2, \end{aligned} \quad (62)$$

i.e. for a force for which the extension $\langle X \rangle$ is of the same order as the coil size $\sqrt{\langle R^2 \rangle_0}$. As one expected for scaling theories, the crossover between the various regimes occur when all characteristic lengths $\sqrt{\langle R^2 \rangle_0}$, $\langle X \rangle$, $\xi_{P,c}$ are of the same order. In the non-linear regime, according to the scaling ansatz, Eq. (11), Eq. (15) gets replaced by (taking $\nu = \frac{2}{3}$ in $d = 3$)

$$\langle X \rangle \propto (k_B T / f \ell_b)^{-2/3} (\ell_p D / \ell_b^2)^{1/3} L, \quad d = 3, \quad (63)$$

or (recall $\nu = 3/4$ in $d = 2$)

$$\langle X \rangle \propto (k_B T / f \ell_b)^{-1/3} (\ell_p / \ell_b)^{1/3} L, \quad d = 2. \quad (64)$$

Thus we see that in the nonlinear regime the persistence of the chains leads to an enhancement of the chain extension by a factor $\ell_p^{1/3}$. Of course, the relation Eq. (64) can only hold if a Pincus blob contains many Kuhn segments, i.e. now $\xi_P = k_B T / f \gg \ell_p$ is required. This condition is nothing but the condition $\langle X \rangle / L \ll 1$, in the case $d = 2$, as expected. In $d = 3$, however, we expect that the Pincus regime, as described by Eq. (63), already ends when the size of a Pincus blob, $\xi_P = k_B T / f$, equals the crossover radius R^* , Eq. (40) (remember that only for radii exceeding R^* the excluded volume effects dominate). For the crossover force

$$f^* = k_B T / R^* \propto k_B T D / \ell_p^2 \quad (65)$$

we find from Eq. (63) that

$$\langle X \rangle / L \propto D / \ell_p \propto f^* \ell_p / k_B T. \quad (66)$$

Comparing Eq. (66) with Eqs. (54), (56), we see that indeed for $f \approx f^*$ a smooth crossover from the Pincus behavior, as described by Eq. (63), to the Kratky-Porod law for wormlike chains for which excluded volume is negligible, can occur. We also note from Eq. (65) that in cases such as occur for bottle brush polymers [43, 44] where chain stiffness is due to chain thickness, $\ell_p \propto D$, we would have $f^* = k_B T / \ell_p$ as in the two-dimensional case, and then the Pincus regime (which applies for $k_B T / \sqrt{\langle R^2 \rangle_0} < f < f^*$) becomes much broader and easier observable.

Finally, we consider again the fluctuations in the extensions of stretched chains (which were considered for flexible chains in Eqs. (20)-(26) already). However, the results known to us for semiflexible chains are somewhat scarce (although the end-to-end distribution function of the Kratky-Porod wormlike chain has been discussed [20, 63-67]). Marko and Siggia [12] obtained for

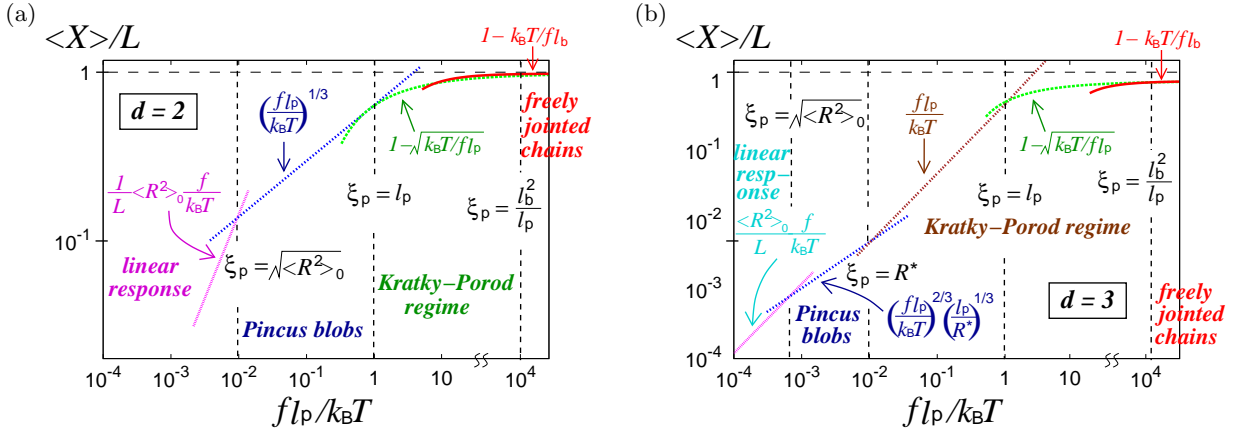


FIG. 1: Schematic plot of the relative chain extension, $\langle X \rangle / L$, versus the scaled force, $(f l_p / k_B T)$, in a log-log scale for $d = 2$ dimensions (a) and $d = 3$ dimensions (b). Broken vertical straight lines indicate various (smooth, not sharp!) crossovers in the response to the stretching force f . The first crossover occurs at very small forces, when the tensile length $\xi_p = k_B T / f$ becomes equal to the chain size $\sqrt{\langle R^2 \rangle_0}$ in the absence of forces. In the first regime (to the left of this crossover) the extension is proportional to the force, $\langle X \rangle \propto \langle R^2 \rangle_0 f / k_B T$ (linear response regime). To the right of this crossover, the extension versus force curve follows the Pincus power law, $\langle X \rangle \propto f^{1/\nu-1} = f^{1/3}$ ($d = 2$) or $\approx f^{2/3}$ ($d = 3$), respectively. In $d = 2$ this power law regime extends up to the crossover where the tensile length equals the persistence length l_p , while in $d = 3$ the power law ends already at an earlier crossover, $\xi_p = R^*$, R^* being the crossover radius where excluded volume statistics comes into play for semiflexible chains: then there exists a regime described by the Kratky-Porod model, $\langle X \rangle / L \propto f l_p / k_B T$. For ξ_p smaller than l_p , the extension approaches saturation according to the Kratky-Porod relation, $1 - \sqrt{k_B T / f l_p}$, while for still larger forces (when the deflection length becomes comparable to the bond length, a further crossover to the behavior expected for freely jointed chains ($\langle X \rangle / L \approx 1 - k_B T / f l_b$)) occurs.

the side-to-side excursions of the chain over a contour length s the result

$$\langle [\vec{r}_\perp(s) - \vec{r}_\perp(0)]^2 \rangle = \frac{2k_B T}{f} \left\{ s l_b - \frac{1 - \exp[-s(f/\kappa k_B T)^{1/2}]}{(f/\kappa k_B T)^{1/2}} \right\} \quad (67)$$

where κ is the coupling constant of the Kratky-Porod model {Eq. (34)}, of course. For $s l_b = L = N_b l_b$ the result $\langle R_\perp^2 \rangle = N_b l_b (2k_B T / f)$ is identical to the large force limit for the flexible chains, Eq. (22). For small s Eq. (67) yields $\langle [\vec{r}_\perp(s) - \vec{r}_\perp(0)]^2 \rangle = s^2 l_b^2 (\kappa k_B T / f)^{1/2}$.

Given the fact that in the Pincus regime the picture of the chain conformation essentially is a stretched string of Pincus blobs (inside a blob excluded volume statistics prevails), we know that there occur of the order of $n = N_b (l_b / l_p) / g$ such blobs per string where g is the number of Kuhn steps (containing l_p / l_b monomers each) per blob. Remember that the Pincus blob has the radius ξ_p , and built as a self-avoiding walk of g steps of length l_p so that $\xi_p = l_p g^\nu$, i.e. $g = (\xi_p / l_p)^{1/\nu} = (k_B T / f l_p)^{1/\nu}$ (here we disregard the factor 2 between the effective Kuhn step length l_k and the persistence length l_p . Thus $n = N_b (l_b / l_p) (f l_p / k_B T)^{1/\nu}$.) If this string of blobs would be completely stretched in a rod-like configuration, its lateral width would be simply $\langle R_\perp^2 \rangle \approx \xi_p^2 = l_p^2 (k_B T / f l_p)^2$. However, this estimate neglects the random statistical fluctuations that the string of blobs may exhibit in the transverse directions. We may consider the problem as a directed random walk where each step

has a component ξ_p in the $+x$ -direction and a transverse component $\pm c \xi_p$, where c is a constant ($c \ll 1$). If we have n such steps ($n = N_b (g l_p / l_b)^{-1}$), we hence predict $\langle R_\perp^2 \rangle = c^2 \xi_p^2 n = c^2 l_p (k_B T / f l_p)^{2-1/\nu} N_b l_b$. Of course, this result can only apply if n is large enough so that $c n^2 > 1$, because $\langle R_\perp^2 \rangle$ cannot be smaller than ξ_p^2 , of course. Hence we would predict from these speculative scaling arguments

$$\langle R_\perp^2 \rangle \propto \xi_p^2 n = l_p l_b N_b (k_B T / f l_p)^{2-1/\nu}, \quad n \rightarrow \infty \quad (68)$$

$$\langle R_\perp^2 \rangle = \xi_p^2 = l_p^2 (k_B T / f l_p)^2, \quad \text{small } n. \quad (69)$$

In $d = 2$, this result should hold up to a force $f = k_B T / l_p$, where $\xi_p = l_p$. Then Eq. (68) predicts $\langle R_\perp^2 \rangle \propto l_p l_b N_b = l_p L$, i.e. there a smooth crossover to the result $\langle R_\perp^2 \rangle \propto k_B T L / f$ derived from Eq. (67) occurs. In $d = 3$, however, Eq. (68) is supposed to hold only for $\xi_p > R^* \propto l_p^2 / D$.

At the end of this section, we summarize our findings for the force extension curves (Fig. 1). The key to identify the various regimes is A COMPARISON OF LENGTHS, namely the “tensile length” $\xi_p = k_B T / f$ needs to be compared to the various characteristic lengths of the unperturbed chain.

The simplest case actually occurs in $d = 2$ (Fig. 1a).

For $\xi_p > \sqrt{\langle R^2 \rangle_0}$ we are in the regime of linear response, the extension $\langle X \rangle$ scales linearly with the force {Eq. (61)}. For $\xi_p \approx \sqrt{\langle R^2 \rangle_0}$ the extension $\langle X \rangle$ and

$\sqrt{\langle R^2 \rangle_0}$ are of the same order, linear response breaks down, and a (smooth!) crossover to the nonlinear Pincus regime occurs, $\langle X \rangle/L \propto (f\ell_p/k_B T)^{1/3}$ {Eq. (64)}. The chain can be viewed as a stretched string of ‘‘Pincus blobs’’ of diameter ξ_P (inside the blobs excluded volume statistics prevails). Near $\xi_P = \ell_p$ the extension $\langle X \rangle$ already is no longer much smaller than the contour length L itself. Only the regime where the extension approaches its saturation value, from $\xi_P = \ell_p$ down to $\xi_P = \ell_b^2/\ell_p$, when the deflection length becomes equal to the bond length, the Kratky-Porod model holds {Eq. (58)}, while for still larger forces (where the deflection length would be less than a bond length) the discreteness of the polymer chain causes a different relation between force and extension {Eq. (7)}, as indicated in the figure. Of course, for flexible chains $\ell_p = \ell_b$ (actually ℓ_p is completely ill-defined then) and the Kratky-Porod regime disappears altogether.

For $d = 3$ dimensions the situation is more complicated, since for semiflexible chains without force another regime appears, for distances in between ℓ_p and $R^* = \ell_p^2/D$, where Gaussian statistics prevails, and this regime finds its correspondence in the force versus extension curve. Thus, for very long semiflexible thin chains there are three regimes, where the force-extension curve exhibits power laws: for very weak forces ($\xi_P > \sqrt{\langle R^2 \rangle_0}$) the linear response regime occurs with $\langle X \rangle \propto \langle R^2 \rangle_0 f/k_B T$ {Eq. (60)}, then a nonlinear regime with $\langle X \rangle/L \propto (f\ell_p/k_B T)^{2/3}(\ell_p/R^*)^{1/3}$ {Eq. (63)} follows for $\sqrt{\langle R^2 \rangle_0} > \xi_P > R^* \propto \ell_p^2/D$, and then the linear regime as described by the Kratky-Porod model follows, $\langle X \rangle/L \propto f\ell_p/k_B T$ {Eq. (56)}, for $R^* > \xi_P > \ell_p$. For $\xi_P < \ell_p$ the approach of $\langle X \rangle/L$ to its saturation value unity proceeds in a similar manner as in $d = 2$ {Eqs. (57), (7)}.

Of course, the description in Fig. 1 contains the force-extension curves of fully flexible polymers as a limiting case: there both R^* and ℓ_p tend to ℓ_b , and the regime where the Kratky-Porod model is applicable gradually disappears. The same statement applies to semiflexible chains in $d = 3$ when stiffness is due to chain thickness, so that R^* tends towards ℓ_p , and the nonlinear Pincus blob regime ($\langle X \rangle/L \propto (f\ell_p/k_B T)^{2/3}$) takes over and holds down to $\xi_P \approx \ell_p$. Conversely, if one considers not very long chains, such that $\langle R^2 \rangle_0 \leq R^{*2}$, the regime dominated by excluded volume effects disappears from the picture, and the Kratky-Porod model description becomes valid down to arbitrarily small forces.

We end this section with several caveats: (i) All crossovers in Fig. 1 are smooth and we do not expect any sharp kinks at the crossover values of ξ_P that are indicated by the vertical broken lines; rather gradual changes will occur on the log-log plot $\langle X \rangle/L$ vs. $f\ell_p/k_B T$, spread out over (at least) a decade in $f\ell_p/k_B T$. Consequently, $\sqrt{\langle R^2 \rangle_0}$ must exceed ℓ_p by four (or more!) decades, in order to resolve the multiple crossovers of Fig. 1 in $d = 3$. (ii) We have disregarded any special structures of the polymer such as α -helices known for proteins,

double helix-portions of copolymers formed from double-stranded DNA and other biopolymers, etc. [68, 69]. Any such special structures of biopolymers will lead to non-universal special features of the force-extension curve, in particular in the regime of rather low forces, but these are outside of consideration here. Rather only a generic description of the universal behavior of very long flexible or semiflexible polymers is within our focus. (iii) Very long polymers exhibiting a (swollen) random coil configuration are expected to contain knots (to precisely define them, one can transform the polymer configuration into a closed loop by adding the end-to-end vector as an extra special bond) [70]. Pulling such a chain at both ends will have the effect that the knots tighten, and the knots can only be made to disappear by moving them to the chain ends. Effects due to knots [71, 72] clearly are beyond the realm of our scaling description (while in the computer simulations presented in Secs. IV-VI knots are automatically included implicitly in our models, though we do not make any explicit attempt to study their effects). In view of all these caveats, the extent to which the scaling theory sketched in Fig. 1 is practically useful is a nontrivial matter.

III. MODEL AND SIMULATION TECHNIQUE

The model that we study in this paper is the classical self-avoiding walk (SAW) [6, 9, 57] on square and simple cubic lattices, where bonds connect nearest neighbor sites on the lattice, and the excluded volume interaction is realized by the constraint that every lattice site can be taken only once by an effective monomer occupying that site. We take the lattice spacing as our unit of length, $\ell_b = 1$. Variable chain stiffness (or flexibility) then is introduced into the model by an energy ϵ_b that occurs for any kink (that is at a right angle and costs ϵ_b).

No energy arises for $\theta = 0^\circ$, of course, and hence in the statistical weight of a SAW configuration on the lattice every kink will contribute a factor $q_b = \exp(-\epsilon/k_B T)$. In the presence of a force f , the potential U written in Eq. (2) yields another factor b^X with $b = \exp(f/k_B T)$ to the statistical weight (as in Sec. II, the force f is assumed to act in the positive x-direction, and X is the x-component of the end-to-end vector \vec{R} of the chain). So the partition function of a SAW with N_b bends ($N_b + 1$ effective monomers) and N_{bend} local bends by $\pm 90^\circ$ is

$$Z_{N_b, N_{\text{bend}}}(q_b, b) = \sum_{\text{config}} C(N_b, N_{\text{bend}}, X) q_b^{N_{\text{bend}}} b^X. \quad (70)$$

We have carried out Monte Carlo simulations applying the pruned-enriched Rosenbluth Method [73–75] (PERM algorithm) using chain lengths up to $N_b = 50000$ in $d = 3$ and $N_b = 25600$ in $d = 2$, varying also the chain stiffness over a wide range ($0.005 \leq q_b \leq 1.0$). As mentioned already in Sec. II {Eq. (36)}, this means that the persistence length ℓ_p varies over about two orders of magnitude

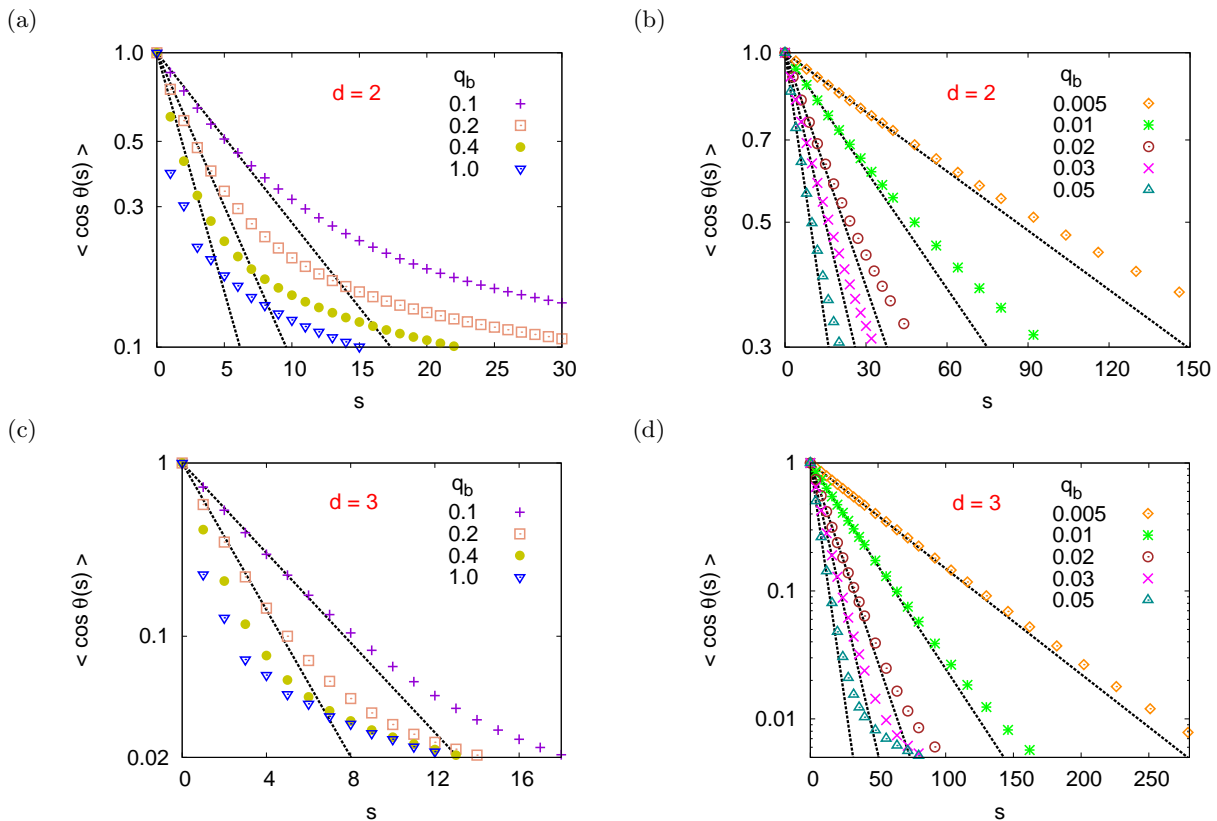


FIG. 2: Semi-log plot of $\langle \cos \theta(s) \rangle$ versus the contour length s , for q_b in the range from $q_b = 0.1$ to $q_b = 1.0$ (a) (c), and for rather stiff chains, $0.005 \leq q_b \leq 0.05$, (b) (d). Data are taken for $N_b = 25600$ in $d = 2$ (a) (b) and for $N_b = 50000$ in $d = 3$ (c) (d). The straight lines indicate fits of the initial decay to Eq. (29), $\langle \cos \theta(s) \rangle \propto e^{-s\ell_b/\ell_p}$; for flexible chains ($q_b = 1.0$ and $q_b = 0.4$) meaningful fits are not possible. Estimates for ℓ_p/ℓ_b are listed in Table I and II. Note the difference in ordinate scales between $d = 2$ and $d = 3$: in $d = 2$, deviations from Eq. (29) have set in when $\langle \cos \theta(s) \rangle$ has decayed to $1/e$, in $d = 3$, however, for very stiff chains one can follow the exponential decay for almost two decades.

(note, however, that in the presence of excluded volume one has to be very careful with the notion of a persistence length, particularly in $d = 2$ dimensions [43–45]).

IV. SEMIFLEXIBLE POLYMERS IN THE ABSENCE OF STRETCHING FORCES

In this section, we summarize our Monte Carlo results for bond orientational correlations and chain linear dimensions obtained for the model described in the previous section. While some of these results have recently been described in our earlier work [43–45], the information provided will be crucial for the understanding of our results for the extension versus force curves as well.

We start with the bond orientational correlation function $\langle \cos \theta(s) \rangle$, Figs. 2-4, since the decay of this function with s is traditionally used to extract “the” persistence length ℓ_p , using Eq. (29). As expected from Sec. II B, however, one must not rely on Eq. (29) to describe the asymptotic decay of $\langle \cos \theta(s) \rangle$ (in the limit where first $N_b \rightarrow \infty$ has been taken, so that one can study large s

without being affected by the finite size of the chain) for large s , but rather one must consider the initial decrease of $\langle \cos \theta(s) \rangle$ with s , cf. Eq. (50). Since $s = 0, 1, 2, 3, \dots$ is a discrete variable, such a fit becomes ill-defined for flexible chains; then the only possible procedure is to use Eq. (30) as a definition of the persistence length, $\ell_{p,\theta} = -\ell_b/\ln[\langle \cos \theta(s = 1) \rangle]$. Both estimates for ℓ_p (from an extended fit over a range of s , and from the latter formula) are collected in Table I, together with the prediction based on Eq. (36), where excluded volume is neglected. One recognizes that Eq. (36) becomes accurate for $d = 3$ as the chains become very stiff, $q_b \rightarrow 0$ while in $d = 2$ Eq. (36) {predicting $\ell_p/\ell_b = 0.5q_b^{-1}$ in this case} never becomes valid. As a consequence, we emphasize that the rule (based on the Kratky-Porod model) that for the same bending stiffness $\kappa/k_B T$ (the continuum analog of our parameter q_b) the persistence length in $d = 2$ is twice as large as in $d = 3$ is not accurate (since this rule fails only by about 24 %, in experimental work where it was tried to extract estimates of ℓ_p from adsorbed semi-flexible chains on two-dimensional substrates this problem was not noticed, due to other

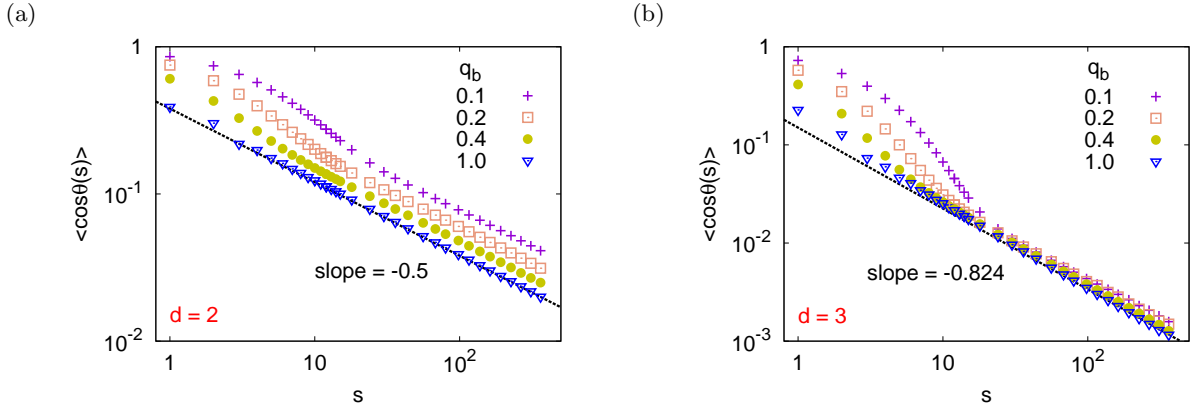


FIG. 3: Log-log plot of $\langle \cos\theta(s) \rangle$ versus s , for $q_b = 0.1, 0.2, 0.4$ and 1.0 , including only data for $N_b = 25600$ in $d = 2$ (a) and for $N_b = 50000$ in $d = 3$ (b). The straight line indicates a fit of the power law, Eq. (49), to the data for $q_b = 1.0$, including only data for $s\ell_b \geq 10$ in the fit, and requesting the theoretical exponent, $\beta = 2 - 2\nu$, with $\nu = 3/4$ in $d = 2$ (a), and $\nu = 0.588$ in $d = 3$ (b).

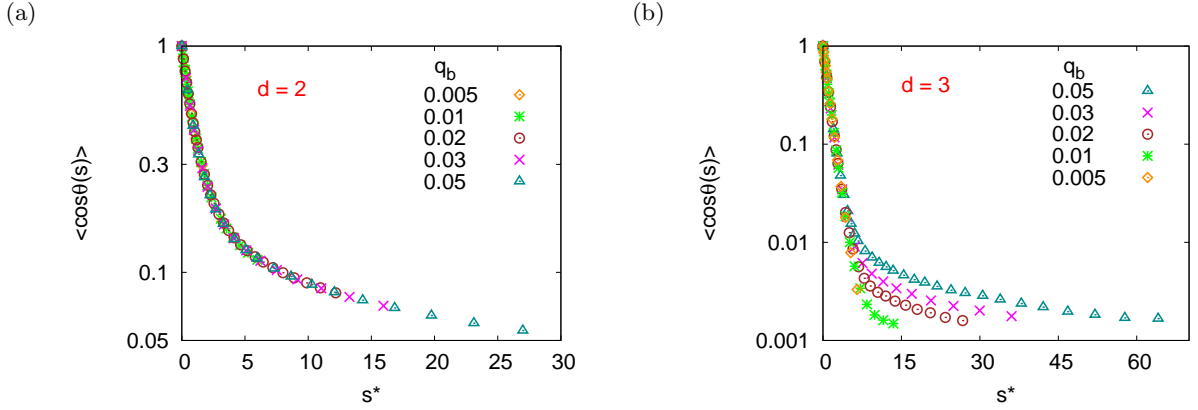


FIG. 4: Semi-log plot of $\langle \cos\theta(s) \rangle$ versus the scaled distance $s^* = s\ell_b/\ell_p$ along the chain, for $d = 2$ (a) and $d = 3$ (b). Data for ℓ_p/ℓ_b extracted from Fig. 2, as described above and listed in Table I and II, were used.

uncertainties in the data analysis).

Fig. 3 plots our data for the bond orientational correlations in a log-log form, to clearly demonstrate that the asymptotic decay is a power law {Eq. (49)} rather than exponential {Eq. (29)}. Eqs. (50), (52) in fact suggest to study $\langle \vec{a}_i \cdot \vec{a}_{i+s} \rangle$ not simply as a function of s but as a function of the rescaled variable $s^* = s\ell_b/\ell_p$. In $d = 2$, one expects a data collapse on a universal master curve and this is indeed found (Fig. 4(a)). No such simple scaling is possible in $d = 3$, however, as expected from Eq. (51).

Another measure of a persistence length in our model is the average number $\langle n_{\text{str}} \rangle$ of successive bonds along the chain that have the same orientation without any kink. The distribution $P(n_{\text{str}})$ of such straight sequences along the chain is plotted in Fig. 5. We find that irrespective of dimensionality and for all values of q_b the distribution shows a simple exponential decay

$$P(n_{\text{str}}) = a_p \exp(-n_{\text{str}}/n_p), \quad (71)$$

and either the average $\langle n_{\text{str}} \rangle = \sum_{n_{\text{str}}=1}^{\infty} P(n_{\text{str}})n_{\text{str}}$ or the decay constant n_p can be taken as a characteristic (similar but not identical to the persistence length) of local intrinsic chain stiffness. Clearly, fitting the data shown in Fig. 5 is less ambiguous than fitting the data for the bond orientational correlations. We also note that $\langle n_{\text{str}} \rangle$ has an obvious physical correspondence in real macromolecules: in alkane-type chains, where the torsional potential has one deeper minimum (the “trans” state, torsional angle $\varphi = 0^\circ$) and two less deep minima (gauche \pm , $\varphi = \pm 120^\circ$) separated from the trans state by high energy barriers, n_{str} simply is the number of successive carbon-carbon bonds in an all-trans configuration. Of course, in this case successive bonds in this state are not oriented along the same direction, since the ground state configuration of the alkanes is a zigzag-configuration, and so Eqs. (29), (50) need to be generalized (bond angles need to be measured relative to their values in the “all-

TABLE I: Various possible estimates for persistence lengths, ℓ_p/ℓ_b from Eq. (29), $\ell_{p,\theta}/\ell_b$ from Eq. (30), n_p and $\langle n_{\text{str}} \rangle$ from Eq. (71) including the fitting parameter a_p , and $\ell_{p,R}/\ell_b$ from Fig. 6, for semiflexible chains in $d = 2$ with various values of q_b .

q_b	0.005	0.01	0.02	0.03	0.05	0.10	0.20	0.40	1.0
ℓ_p/ℓ_b	123.78	62.20	31.36	21.55	13.41	7.53	4.16	2.67	-
$\ell_{p,\theta}/\ell_b$	118.22	59.44	30.02	20.21	12.35	6.46	3.50	2.00	1.06
a_p	0.009	0.017	0.034	0.051	0.085	0.168	0.331	0.646	1.539
n_p	116.34	58.81	29.78	20.07	12.28	6.44	3.50	2.01	1.08
$\langle n_{\text{str}} \rangle$	118.06	59.78	30.48	20.69	12.85	6.97	4.02	2.54	1.64
$\ell_{p,R}/\ell_b$	3.34	2.37	1.70	1.39	1.09	0.81	0.61	0.48	0.39

TABLE II: Various possible estimates for persistence lengths, ℓ_p/ℓ_b from Eq. (29), $\ell_{p,\theta}/\ell_b$ from Eq. (30), n_p and $\langle n_{\text{str}} \rangle$ from Eq. (71) including the fitting parameter a_p , and $\ell_{p,R}/\ell_b$ from Ref. [44], for semiflexible chains in $d = 3$ with various values of q_b .

q_b	0.005	0.01	0.02	0.03	0.05	0.10	0.20	0.40	1.0
ℓ_p/ℓ_b	52.61	26.87	13.93	9.54	5.96	3.35	2.05	-	-
$\ell_{p,\theta}/\ell_b$	51.52	26.08	13.35	9.10	5.70	3.12	1.18	1.12	0.67
a_p	0.02	0.04	0.08	0.12	0.19	0.38	0.73	1.42	3.37
n_p	51.17	25.95	13.30	9.07	5.68	3.12	1.82	1.13	0.68
$\langle n_{\text{str}} \rangle$	51.72	26.50	13.83	9.60	6.20	3.65	2.36	1.70	1.29
$\ell_{p,R}/\ell_b$	5.35	3.49	2.39	1.94	1.54	1.12	0.87	0.71	0.61

trans" configuration). Similarly in biopolymers a sequence of n_{str} bonds in an α -helix configuration can be the right object to characterize stiffness. Such considerations will be needed when one wants to adapt our findings to real polymer chains. Finding an analogue of Eq. (71) that is generally valid for off-lattice models is in interesting problem but beyond the scope of the present study.

We now turn to the end-to-end distance of the chains (Figs. 6, 7). As predicted by the theoretical considerations of Sec. II, we find in $d = 2$ and $d = 3$ dimensions very different behaviors. In $d = 2$ (Fig. 6) the data for small enough N_b show the rod-like behavior, $\langle R_e^2 \rangle \propto N_b^2$, indicated by the slope of the straight line in the left of Fig. 6(a), (b), and then $\langle R_e^2 \rangle \propto N_b^{2\nu}$ with $\nu = 3/4$ reaches a broad maximum, and thereafter decreases only a little bit and then settles down at the limiting value expected for two-dimensional self-avoiding walks. As the rescaled plot (Fig. 6(b)) shows, there is a single crossover from rods to self-avoiding walks, and irrespective of stiffness there is never a regime where the Gaussian plateau predicted by the Kratky-Porod model {Eq. (32)} describes part of the data approximately. Of course, the latter can describe the initial rod-like behavior [49] but this is of little interest and clearly from this regime one cannot estimate ℓ_p reliably at all. Interestingly we find from the rescaled plot (Fig. 6(b)) that the maximum which appear at $N_b = N_b^{\text{max}}$ in Fig. 6(a) rather accurately coincides with the value $N_b = N_b^*$, the chain length corresponding to the effective Kuhn length $\ell_k = 2\ell_p$. As an immediate consequence of this finding we can suggest as a recipe for experimentalists who analyze end-to-end-distances of two-dimensional adsorbed chains to plot their data in

analogy to Fig. 6(a)): if their chain lengths N_b are long enough to reach the region where the maximum N_b^{max} in such a plot occurs, they can immediately estimate the persistence length as

$$\ell_p = \ell_b N_b^{\text{max}} / 2. \quad (72)$$

For this method to work, it is not necessary at all to have chains long enough to see the asymptotic $d = 2$ SAW behavior, $\langle R_e^2 \rangle \propto N_b^{3/2}$. Since the Kratky-Porod model {Eq. (32)} has so widely been used by experimentalists to fit their data and by theorists to build more sophisticated extensions on it, we emphasize again that Eq. (32) is accurate only in the rod-like regime and in the initial part of the crossover towards the self-avoiding walk regime as shown in Fig. 6(b). Note that unlike experimental work, this comparison does not involve any adjustable parameter whatsoever. We see that for small N_b and small q_b theory and simulation agree qualitatively, but in this regime, where curves for small N_b collapse on the straight line $\langle R_e^2 \rangle / \ell_b N_b = \ell_b N_b$, and then gradually bend over to a slower increase, the data are not very sensitive to the actual value of ℓ_p . For $N_b < 2N_b^*$ the Kratky-Porod result slightly overestimates the actual data, while for $N_b \gg 2N_b^*$ it strongly underestimates them, since the increase proportional to $\langle R_e^2 \rangle \propto N_b^{3/2}$ cannot be described. Clearly, the plateaus predicted by Eq. (32) for $N_b > 2N_b^*$, as displayed in Fig. 6(b), do not have any correspondence to the actual data.

However, in the three-dimensional case the situation is clearly different [43, 44]. We shall not reproduce in full detail the data published already elsewhere [43, 44] but only show as a summary of the scaling plots in the

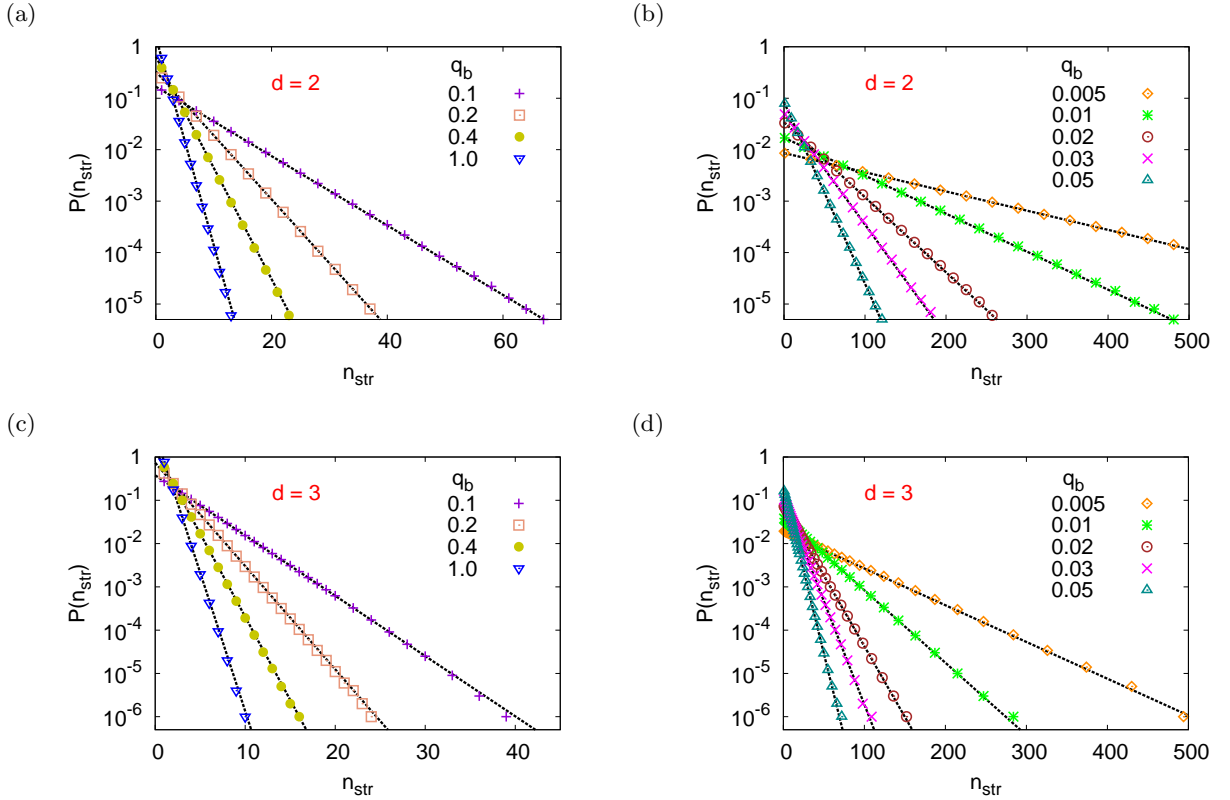


FIG. 5: Semi-log plot of the distribution $P(n_{\text{str}})$ of n_{str} successive bonds along the chain which continue straight along a lattice direction until a kink appears, versus n_{str} for rather flexible chains, i.e. $0.1 \leq q_b \leq 1.0$ in $d = 2$ (a) and $d = 3$ (c), as well as for rather stiff chains, i.e. $0.005 \leq q_b \leq 0.05$, in $d = 2$ (b) and $d = 3$ (d). The straight lines indicate fits to simple exponential functions, Eq. (71), $P(n_{\text{str}}) = a_p \exp(-n_{\text{str}}/n_p)$, with constants a_p and n_p quoted in Table I and II. All data are taken for $N_b = 25600$ in $d = 2$ and $N_b = 50000$ in $d = 3$.

Kratky-Porod representation for the three-dimensional cases (Fig. 7). Now there is clear evidence from the data (Fig. 7(a)) that with increasing stiffness (decreasing q_b) a Gaussian plateau in the plots of $\langle R_e^2 \rangle / (2\ell_b N_b \ell_p)$ versus $N_b / N_b^{\text{rod}}(q_b)$ develops, before the regime ruled by excluded volume interactions sets in. Here we rescale the chain length N_b such that data collapse occurs in the rod-like regime, i.e. N_b is rescaled with $N_b^{\text{rod}} = 2\ell_p / \ell_b$. We see that with increasing ℓ_p the data gradually approach the Kratky-Porod result {Eq. (32)} over an increasing range of N_b / N_b^{rod} , while ultimately the data increase beyond the Kratky-Porod plateau values, to cross over to the asymptotic relation $\langle R_e^2 \rangle / N_b \propto N_b^{2\nu-1}$ as it should be {compare Eqs. (39)-(43)}. Alternatively, we can estimate another crossover chain length $N_b^*(q_b)$ such that the curves collapse in the regime of large N_b , so that the asymptotic regime where excluded volume interactions dominate, shows proper scaling behavior (Fig. 7b). Obviously, while in $d = 2$ dimensions $N_b^*(q_b) = N_b^{\text{rod}}(q_b)$, so there is no need to distinguish these crossover chain lengths at all, (Fig. 6b), and there is a single crossover from rods to self-avoiding walks described by one universal crossover scaling function, this is not true in $d = 3$

dimensions: there occur two successive crossovers, from rods to Gaussian coils at $N_b = N_b^{\text{rod}}$, and from Gaussian coils to three-dimensional self-avoiding walks, at $N_b = N_b^*$. Of course, these crossovers are rather gradual and not sharp: therefore a well-defined Gaussian plateau comes into existence only for $N_b^* \gg N_b^{\text{rod}}$, which requires extremely stiff chains. These findings are in beautiful qualitative agreement with the theoretical considerations of Sec. II B and with available experiments in $d = 3$ that did show two successive crossovers [60]. Surprisingly, some authors [76] claim to have observed two successive crossovers (with an intermediate Gaussian regime) for two-dimensional adsorbed chains. We suspect that the observations may be due to incomplete equilibration of the chains, and we feel that the theoretical interpretation given there is inappropriate, however.

It remains to test to what extent the predictions given in Sec. II B for the crossover chain lengths N_b^{rod}, N_b^* are actually compatible with our data. First of all, Fig. 8(a) illustrates that both in $d = 2$ and $d = 3$ the region where ℓ_b follows the simple asymptotic power law $\ell_b \propto q_b^{-1}$ is quickly reached, and we have ample data where ℓ_p exceeds ℓ_b by at least an order of magnitude.

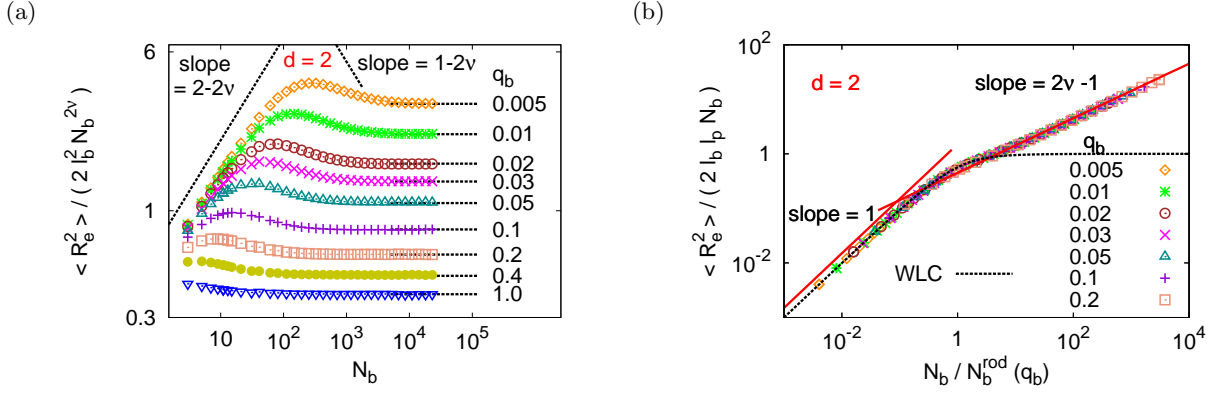


FIG. 6: Log-log plot of the rescaled mean square end-to-end distance in $d = 2$ dimensions, $\langle R_e^2 \rangle / (2 \ell_b^2 N_b^{2\nu})$ with $\nu = 3/4$, versus N_b (a) and the normalized rescaled mean square end-to-end distance $\langle R_e^2 \rangle / (2 \ell_b \ell_p N_b)$ versus rescaled chain length N_b / N_b^{rod} (b). These data include chain lengths N_b up to $N_b = 25600$, and all values of the stiffness parameter q_b , as indicated. Straight lines in (a) show the slope $2 - 2\nu = 0.5$ describing the rod-like regime (that occurs for small N_b) and the slope $1 - 2\nu = -0.5$ that would occur if a Gaussian-like regime was present (which is not). Dotted horizontal plateaus for large N_b in (a) show estimates for $\ell_{p,R}(q_b)/\ell_b$ (Table I). Part (b) shows that all data collapse to a single master curve which describes a crossover from a rod-like regime to a self-avoiding walk regime. The Kratky-Porod function, Eq. (32), indicated by the dotted curve (WLC) is also shown for comparison. The chain length $N_b^* = N_b^{\text{rod}} = \ell_k/\ell_b = 2\ell_p/\ell_b$ describing the number of bonds per effective Kuhn segment ℓ_k is extracted from the persistence length estimates (Table I).

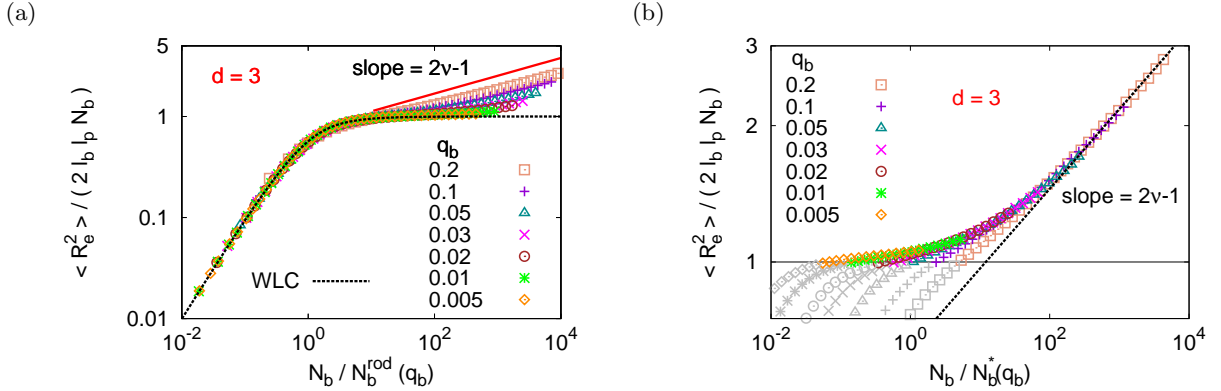


FIG. 7: Log-log plot of $\langle R_e^2 \rangle / (2 \ell_b \ell_p(q_b) N_b)$ versus $N_b / N_b^{\text{rod}}(q_b)$ with $N_b^{\text{rod}} = 2\ell_p(q_b)/\ell_b$. As always, $\ell_p(q_b)/\ell_b$ is extracted from the initial decay of the bond vector correlation function (Fig. 2 and Table II). Now the initial part of the data scale, and the smaller q_b (increasing ℓ_p) the more the data follow the Kratky-Porod function, Eq. (32), indicated by the dotted curve labeled WLC. Part(b) shows the same data but plotted versus $N_b / N_b^*(q_b)$ (a) where $N_b^*(q_b)$ is defined such that for large N_b an optimal data collapse on the straight line representing the three-dimensional self-avoiding walk behavior $\langle R_e^2 \rangle \propto N_b^{2\nu}$ is obtained. Note that data that fall below the Kratky-Porod plateau (horizontal straight line) for different stiffness parameters systematically splay out, there is no scaling over the full parameter range.

Fig. 8b also illustrates that in the case of a single crossover Eq. (47) is quantitatively verified, since Eq. (47) says $R^2 \propto \ell_k^{1/2} L^{3/2} = \ell_b^{3/2} \ell_k^{1/2} N_b^{3/2}$, and hence using $\langle R_e^2 \rangle = 2\ell_{p,R} \ell_b N_b$ we would conclude $\ell_{p,R} = (\ell_p \ell_b)^{1/2} / \sqrt{2}$, if the proportionally constant in Eq. (47) is taken to be unity. Of course, only the exponent in this relation and not the prefactor can be taken seriously. However, in $d = 3$ the theoretical relations $N_b^* \propto \ell_p^3$ and $\ell_{p,R} \propto \ell_p^{2/5}$ {Eqs. (40), (43)} are not quantitatively ver-

ified: rather we found effective exponents $\ell_{p,R} \propto \ell_p^{0.56}$ and $N_b^* \propto \ell_p^{2.5}$ (Fig. 8c). We cannot rule out that this result is due to a still somewhat slower crossover to the asymptotic excluded volume dominated regime than assumed in our fit in Fig. 7; still much longer chains than $N_b = 50000$ would be needed to check this, but this is a very tough task even for the PERM algorithm. On the other hand, we note that Eqs. (38)-(43) clearly are not exact, the Flory argument invariably implies that $\nu = 3/5 = 0.60$ instead of $\nu = 0.588$ [52] and it is un-

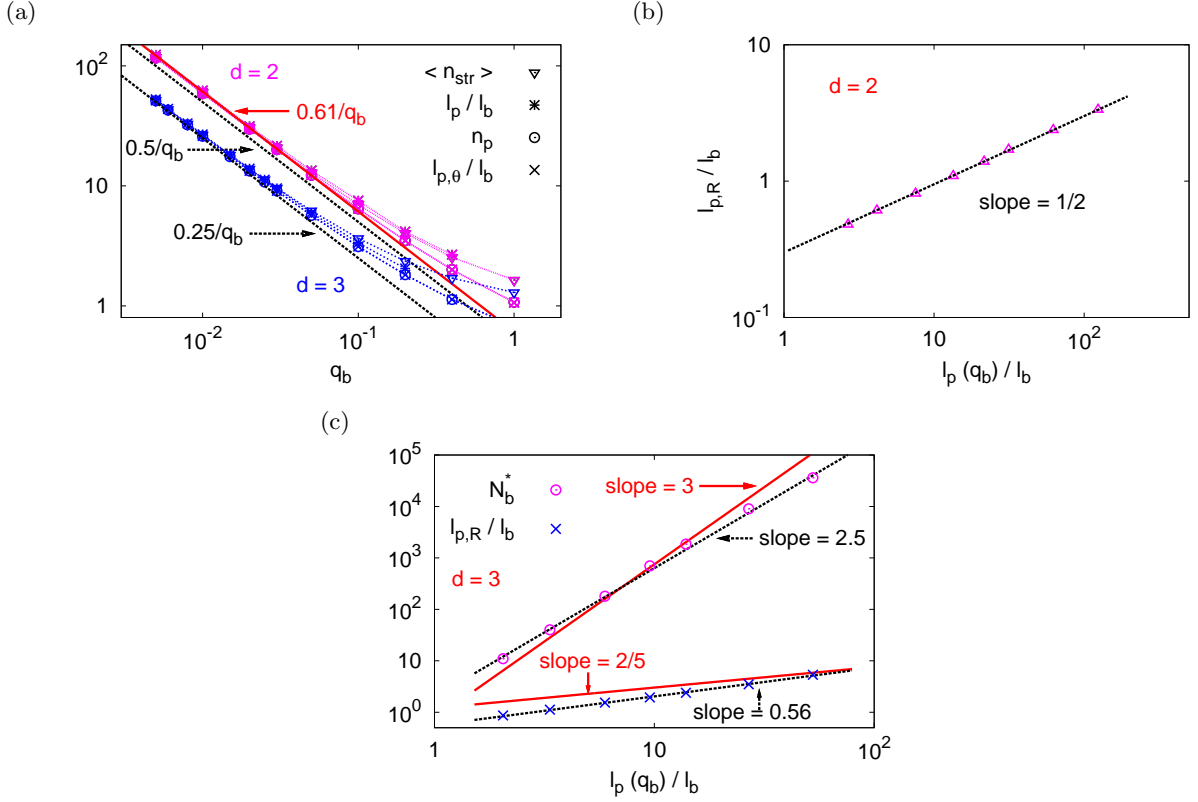


FIG. 8: Log-log plot of various possible estimates for a persistence length ℓ_p plotted vs. q_b in both $d = 2$ and $d = 3$, as indicated. Here n_p and $\langle n_{\text{str}} \rangle$ are extracted from the use of Eq. (71), cf. Fig. 5, while ℓ_p/ℓ_b is taken from the fit to the initial decay of $\langle \cos \theta(s) \rangle$ with s , and $\ell_{p,\theta}/\ell_b$ is taken directly from $\langle \cos \theta(s=1) \rangle$ ($\ell_{p,\theta} = -\ell_b / \ln([\langle \cos \theta(s=1) \rangle])$). (b) Log-log plot of the amplitude $\ell_{p,R}/\ell_b$ characterizing the prefactor of the asymptotic excluded volume region, $\langle R_e^2 \rangle = 2\ell_b \ell_p n_p N^{2\nu}$ with $\nu = 3/4$, in $d = 2$, versus $\ell_p(q_b)/\ell_b$. Straight line shows a fit to $\ell_{p,R}/\ell_b = 0.3(\ell_p/\ell_b)^{1/2}$. (c) Log-log plot of $\ell_{p,R}/\ell_b$ and N_b^* in $d = 3$ dimensions versus ℓ_p/ℓ_b , as extracted from the fit shown in Fig. 7. Both effective exponents and theoretical power laws are indicated (cf. text).

clear to us to what extent these exponents describing the variation of $\ell_{p,R}$ and N_b^* with ℓ_p are modified. This problem could possibly be addressed with the renormalization group approach.

V. STRETCHING SEMIFLEXIBLE POLYMERS IN $d = 2$ DIMENSIONS

Fig. 9 presents now a selection of our results for extension versus force curves for the two-dimensional SAW's of variable stiffness on a square lattice. As expected, neither the simple result for freely jointed chains {Eq. (4)} nor the Kratky-Porod result {Eq. (55)} are compatible with the data. For very short chains ($N_b = 100$) and intermediate values of the stiffness ($q_b = 0.05$ which corresponds to $\ell_p \approx 13\ell_b$, cf. Table I) we note that $\langle X \rangle/L$ roughly agrees with Eq. (55), however: this agreement probably is not accidental, since also in the absence of a force for such short chains and this choice of q_b the Kratky-Porod prediction for the mean square end-to-end

distance (Fig. 6(b)) still is rather close to the actual result for $\langle R_e^2 \rangle / 2\ell_p L$. Similar agreement was also noted in our earlier work [45] for somewhat longer and stiffer chains ($N_b = 200$ and $q_b = 0.03$ and 0.02 , respectively) for exactly the same reason: as long as $\langle R_e^2 \rangle$ in the absence of forces is still more or less correctly predicted, and this can be judged from the data presented in the previous section, the general linear response relation, Eq. (9), which holds not only for flexible SAW's but also for stiff chains, implies that the K-P model still provides an accurate description of the initial linear part of the extension versus force curve. Since in such a case where L is larger than ℓ_p by only a small factor, beyond the linear response regime there is no regime of Pincus blobs possible, since $\sqrt{\langle R^2 \rangle_0}$ in Fig. 1(a) and ℓ_p then are of the same order (each Pincus blob needs to be formed from many subunits of size ℓ_p , in order that the power law regime $\langle X \rangle/L \propto (f\ell_p/k_B T)^{1/3}$ can develop!) Thus, we arrive at the general conclusion that in $d = 2$ the K-P result Eq. (55), is applicable only for such short chains that L is larger than ℓ_p by only a small factor ($L \leq 10\ell_p$, say),

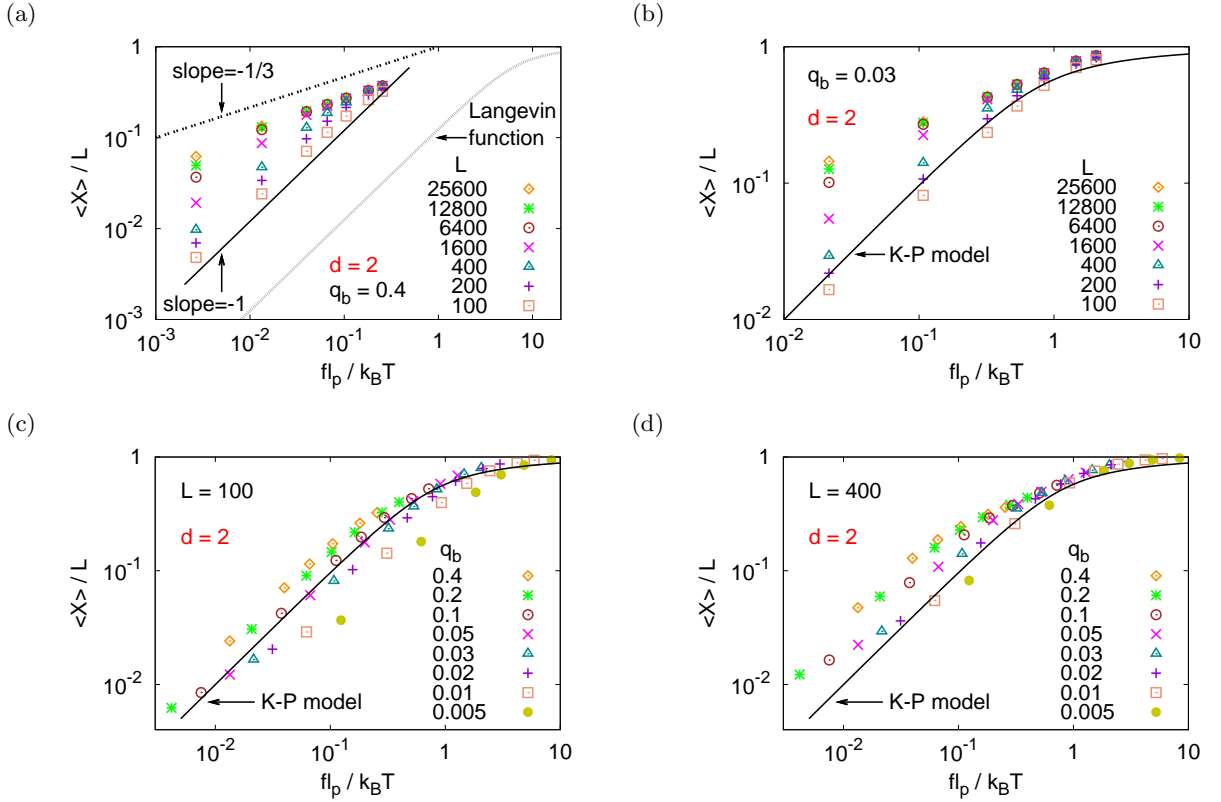


FIG. 9: Relative extension $\langle X \rangle / L$ plotted versus scaled force $f \ell_p / k_B T$ for rather flexible chains ($q_b = 0.4$, case (a)) and for rather stiff chains ($q_b = 0.03$, case (b)) in $d = 2$, including several different contour lengths $L = N_b \ell_b$, as indicated. In (a), the prediction Eq. (4), $\langle X \rangle / L \propto \mathcal{L}((f \ell_p / k_B T)(\ell_b / \ell_p))$, for the freely jointed chain and Eq. (63) for the Pincus blob prediction are included for comparison, while in (b) the result Eq. (55) for the Kratky-Porod model is included. Note that in (a) the result $\ell_p = 2.67 \ell_b$ (Table I) was used to convert the scale from $f \ell_p / k_B T$ to $f \ell_b / k_B T$. Case (c) plots $\langle X \rangle / L$ versus $f \ell_p / k_B T$ and variable q_b (and hence variable ℓ_p , cf. Table I) for $L = 100$ and case (d) for $L = 400$, respectively. Eq. (55) is again included for comparison.

so that in Fig. 1(a) the Pincus blob regime is essentially absent, and the K-P model also achieves an approximate description of the linear response regime.

Of course, it is of great interest to clarify what happens when $L \gg \ell_p$. Fig. 10 hence presents a log-log plot of the data for the extension versus force curves including long chains and rescaling the data such that a scaling description for the crossover from the linear response to the regime of Pincus blobs is obtained. One sees that both for flexible chains (Fig. 10(a)) and for rather stiff chains (Fig. 10(b)) a reasonable data collapse on a master curve is obtained, consistent with the predicted exponents. As expected, the crossover between both power laws is gradual and not sharp. If one includes data for too large forces, one can see that the data fall systematically below the Pincus power law. Similarly, when one puts the focus on the crossover from the Pincus blob regime to the saturation behavior, Fig. 10(c), one finds that the data fall systematically below the Pincus power law for small forces (due to the crossover towards the linear response regime). As expected from the theoretic-

cal considerations of Sec. II, there cannot exist a scaling representation which brings both crossovers of Fig. 1(a) to a data collapse on a master curve together. Note also that for the long chains the K-P model does not fit our data at large relative extensions $\langle X \rangle / L$ either, since our simulations are based on a discrete chain model. Since our choices of q_b do not yield extremely large persistence lengths, the crossover from the saturation behavior predicted by the K-P model {Eq. (58)} to that of the FJC model {Eq. (7)} is not clearly resolved either. Actually, for very large forces one must consider that our model is a lattice model, not a model of rigid bonds in the continuum where arbitrary bond angles occurs such as the FJC model: hence we expect that for $f \rightarrow \infty$ the saturation behavior is $1 - \langle X \rangle / L \propto \exp(-f \ell_b / k_B T)$ rather than $k_B T / f \ell_b$.

As a last point of this section, we consider both longitudinal (Fig. 11(a)(b)) and transverse (Fig. 11(c)(d)) fluctuations of the chain dimensions. These fluctuations have been normalized such that they are of order unity (and independent both L and ℓ_p) in the lin-

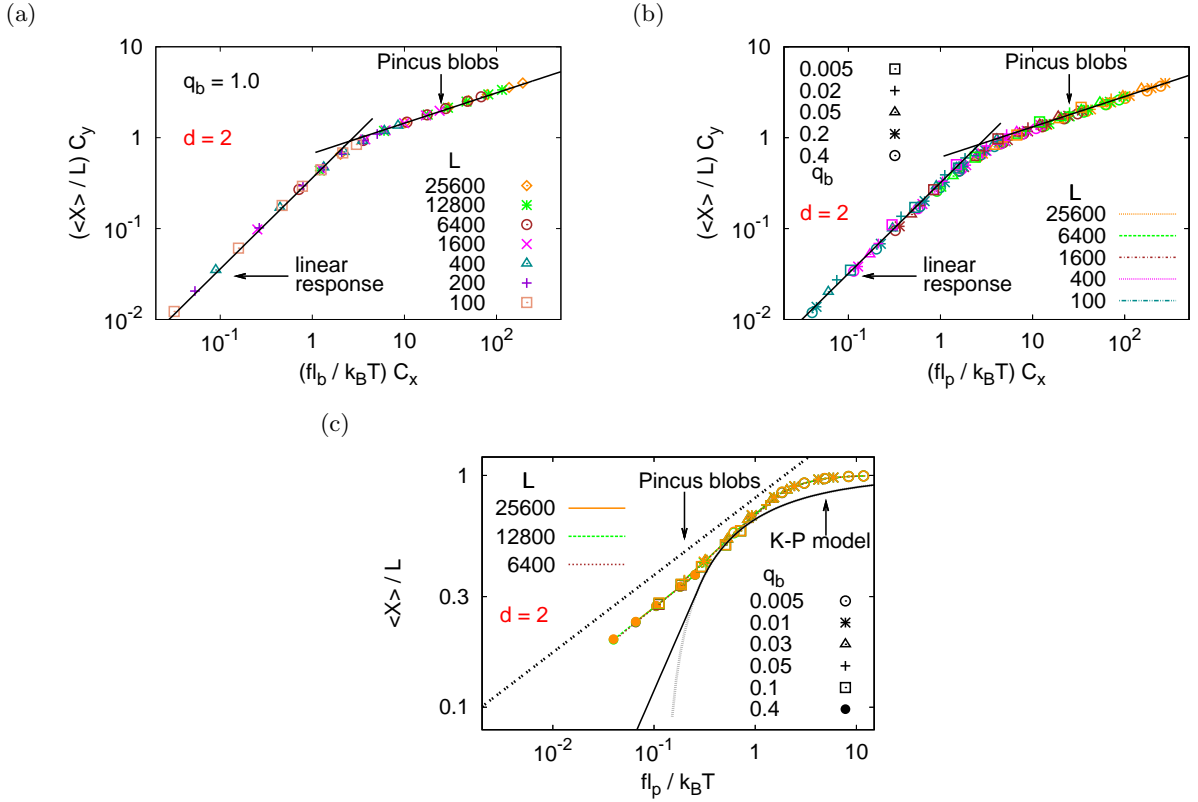


FIG. 10: Plot of $y = (\langle X \rangle / L) C_y$ versus $x = (f \ell_b / k_B T) C_x$ for flexible SAW's in $d = 2$ ($q_b = 1$) where the scaling factors C_x, C_y for abscissa and ordinate have been chosen $C_x = N_b^{3/4}, C_y = N_b^{1/4}$, so that the coordinates (x_{cr}, y_{cr}) of the crossover point from the linear response regime to the Pincus blob regime in the (x, y) plane are of order unity. Several choices of L are included, as indicated. Part (b) is similar as (a), but for semiflexible chains with several choices of q_b and L , as indicated. Now $x = (f \ell_p / k_B T) C_x$ and the scaling factors are chosen as $C_x = (L / \ell_p)^{3/4}, C_y = (L / \ell_p)^{1/4}$. Straight lines in both parts indicate the theoretical power law $\langle X \rangle \propto f$ (linear response regime) and $\langle X \rangle \propto f^{1/3}$ (Pincus blobs regime), respectively. Part (c) is the same as (b), but choosing $C_x = C_y = 1$ including only data for $L = 25600, 12800,$ and 6400 , to show the crossover from the Pincus blob regime to a Kratky-Porod (K-P) like regime.

ear response regime, while in the Pincus blob regime ($0 \ll f \ell_p / k_B T < 1$) a crossover to a simple power law proportional to $(f \ell_p / k_B T)^{1/\nu-2}$ occurs. Using the same scaling factors $C_x = (L / \ell_p)^{3/4}$ (Fig. 10(b)) for abscissa, a nice data collapse on the master curve is seen in Fig. 12 for both longitudinal and transverse fluctuations. Note that our scaling description for the crossover from the linear response regime to the Pincus blob regime, exemplified in Fig. 10 and 12, does not invoke any adjustable parameters whatsoever (unlike the case of experiments, where often both L and ℓ_p are fit parameters). However, the behavior at larger forces (beyond Pincus blob regime) is more subtle. While in the Kratky-Porod regime a power law proportional to $(f \ell_p / k_B T)^{-2}$ is expected for large enough f , where a behavior similar as that has been found for freely jointed chains {Eq. (21)} can be expected, when one considers the longitudinal fluctuation $\{(\langle X^2 \rangle - \langle X \rangle^2) / \langle X^2 \rangle_0\}$, for the transverse fluctuation $\langle R_\perp^2 \rangle / \langle R_\perp^2 \rangle_0$ all theories predict a slower decay (proportional to $[(f \ell_p / k_B T)^{-1}]$ for large f {Eqs. (22), (24),

and (67), respectively}), and this slower decay in fact is not seen. The reason for this discrepancy, however, probably is the fact that in our model only kinks by $\pm 90^\circ$ are possible, and no small deflections are possible as in the K-P and FJC models. We defer a more detailed analysis of these fluctuations to a forthcoming publication. Here we rather focus on the behavior of the local angular fluctuation $\langle \phi^2 \rangle$ (Fig. 13). For small forces all angles ϕ between a bond and the $+x$ -direction are equally probable (at the lattice we have in $d = 2$ two possibilities for $\phi = \pi/2$ or $\phi = -\pi/2$, and two possibilities for $\phi = 0$ or π , respectively). Hence for $f \rightarrow 0$ we must find $\langle \phi^2 \rangle = (\pi^2 + \pi^2/2)/4 = 3\pi^2/8 \approx 3.7$, and this is compatible with the observation. For $f \ell_p / k_B T > 1$ we observe a smooth crossover towards

$$\langle \phi^2 \rangle \propto k_B T / (f \ell_p), \quad f \ell_p \gg k_B T \quad (73)$$

and the crossover from $\langle \phi^2 \rangle \approx 3.7$ to this decay seems to be practically independent of ℓ_p (as shown by the superposition of data for different choices of q_b and hence ℓ_p

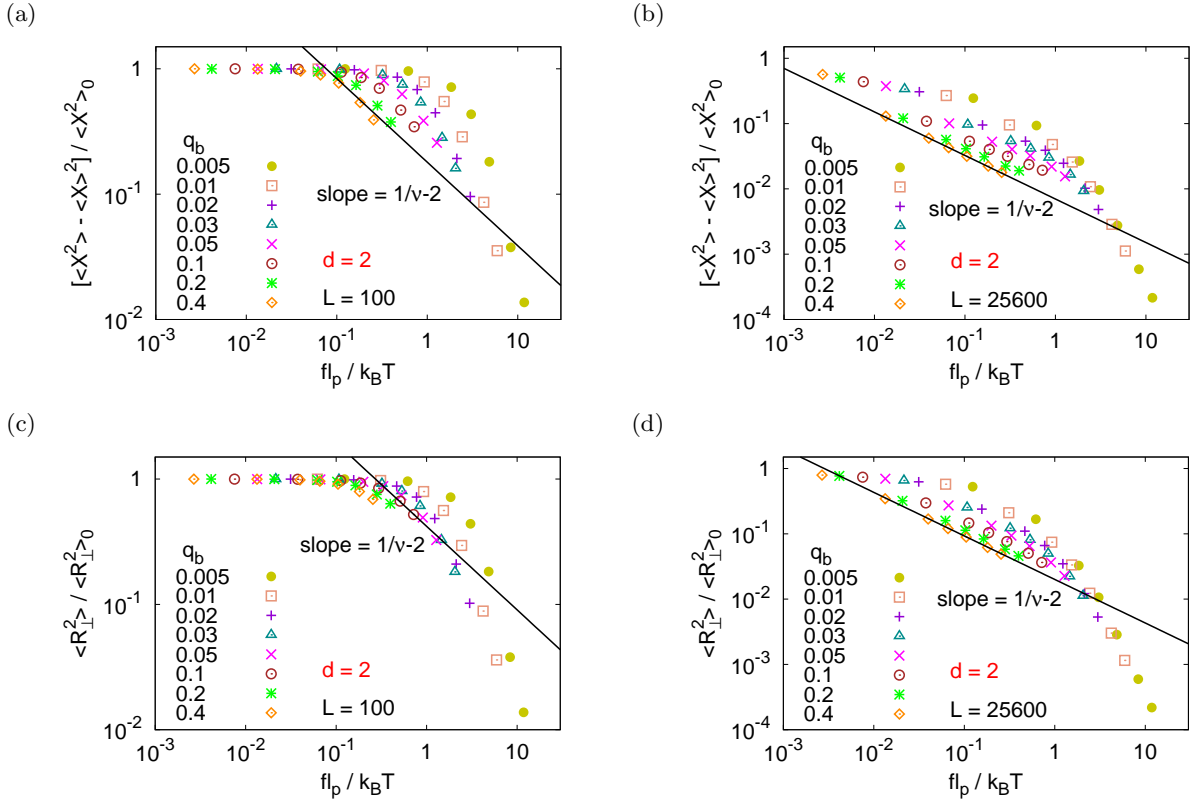


FIG. 11: Log-log plot of $[\langle X^2 \rangle - \langle X \rangle^2] / \langle X^2 \rangle_0$ vs. $fl_p / k_B T$ for $L = 100$ (a), and $L = 25600$ (b), including several choices for q_b as indicated. Log-log plot of $\langle R_{\perp}^2 \rangle / \langle R_{\perp}^2 \rangle_0$ vs. $fl_p / k_B T$ for $L = 100$ (c) and $L = 25600$ (d), including several choices for q_b as indicated. A straight line with slope $1/\nu - 2$ ($\nu = 3/4$) is shown for comparison. Data are for semiflexible chains in $d = 2$.

in Fig. 13) and L (compare Fig. 13(a) for $L = 100$ with Fig. 13(b) for $L = 25600$). Although the local quantity $\langle \phi^2 \rangle$ thus has a remarkably simple behavior, unlike the global quantities $\langle X \rangle / L$, $(\langle X^2 \rangle - \langle X \rangle^2) / \langle X^2 \rangle_0$ and $\langle R_{\perp}^2 \rangle / \langle R_{\perp}^2 \rangle_0$, we are not aware of any theoretical prediction relating to it.

VI. STRETCHING SEMIFLEXIBLE POLYMERS IN $d = 3$ DIMENSIONS

We start by showing extension versus force curves for various choices of the contour length L in Fig. 14, to provide a three-dimensional counterpart to the data in Fig. 9 for two dimensions. It is immediately obvious that the simple Kratky-Porod prediction {Eq. (54)} does a much better job than its two-dimensional counterpart {Eq. (55)}. Again, we emphasize that there are no adjustable parameters whatsoever in our comparison, $L = N_b \ell_b$ is trivially known, and ℓ_p comes from Fig. 2(d). In fact, for $L = 200$ and $L = 400$ most of the data for $0.01 < \langle X \rangle < 0.3$ follow the K-P prediction, for a wide range of choices for q_b and hence ℓ_p {Table II}, only data for rather flexible chains (such as $q_b = 0.4$, for which $\ell_p = 1.2$) deviate strongly from the K-P model, as ex-

pected. The simple Langevin function {Eq. (4)} does not describe the behavior of these lattice chains with discrete bond angles. Note that these chains are too short to show a well-developed Pincus blob regime yet. For $\langle X \rangle / L > 0.3$ systematic deviations from the K-P prediction occur, which we attribute to effects due to the discreteness of bonds and bond angles in our model. Only for very long chains (such as $N = 6400$ and 25600) do we find more pronounced deviations from the K-P prediction also for small relative extensions, $\langle X \rangle / L \leq 0.1$.

For long chains, however, we do expect to see excluded volume effects (manifested in Pincus blobs), as discussed in Sec. II. Thus Fig. 15 presents our data in suitably scaled form, considering the crossover from the linear response regime to the Pincus blob regime, both for flexible chains (a) and semiflexible ones (b), as well as the crossover from Pincus blobs to Kratky Porod behavior (c), and we show a close-up of the Kratky-Porod regime for very long and at the same time rather stiff chains (d). Of course, even with chain lengths up to 25600 it is not yet possible to clearly resolve all the different power laws shown in Fig. 1 (b): in order to be able to distinguish the various crossovers clearly from each other, we would need very stiff chains (ℓ_p should then be in the range $10^2 < \ell_p / \ell_b < 10^4$), and then one would

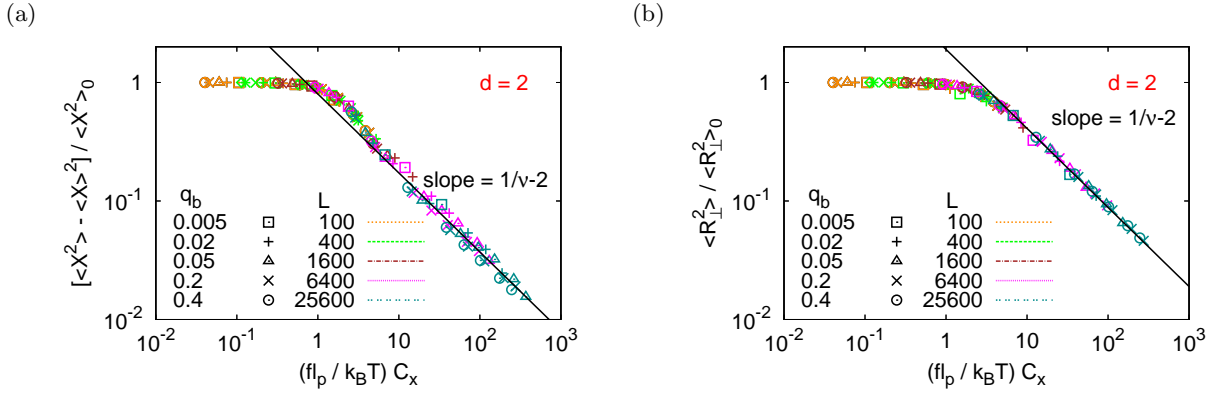


FIG. 12: Log-log plot of $[\langle X^2 \rangle - \langle X \rangle^2] / \langle X^2 \rangle_0$ (a) and $\langle R_{\perp}^2 \rangle / \langle R_{\perp}^2 \rangle_0$ (b) vs. $(f\ell_p/k_B T) C_x$ with $C_x = (L/\ell_p)^{3/4}$ (see Fig. 10(b)) for semiflexible chains in $d = 2$ including several choices of L and q_b , as indicated.

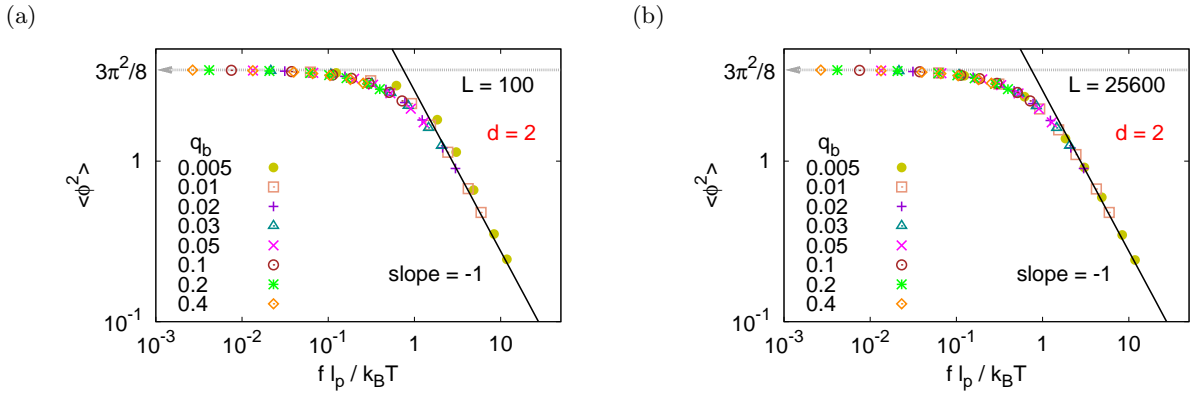


FIG. 13: Log-log plot of $\langle \phi^2 \rangle$ vs. $f\ell_p/k_B T$ for $L = 100$ (a), and $L = 25600$ (b), including several choices for q_b as indicated. $\langle \phi^2 \rangle = 3\pi^2/8$ as $f \rightarrow 0$. Data are for semiflexible chains in $d = 2$.

need to have chain lengths of many millions in order to have a well-developed Pincus-blob regime. Thus, we can verify the Pincus blob regime only for rather flexible chains (Fig. 15(a)), for which then a well-developed Kratky-Porod regime is absent. For the stiff chains, we can see some tendency of the data to deviate from the K-P regime in the direction towards the Pincus blob regime (Fig. 15(b)(c)), but the latter is not fully reached because the crossover to the linear response takes over (Fig. 15(b)). And when we study very stiff chains, we find deviations from the K-P model for rather small $\langle X \rangle / L$ already, due to the discrete character of our chains.

Fig. 16 shows again data for the normalized fluctuations of the chain linear-dimensions, and Fig. 17 presents a counterpart to Fig. 13, showing a log-log plot of the local fluctuation $\langle \phi^2 \rangle$ versus $f\ell_p/k_B T$. While the latter (for large L) show again a simple crossover from the constant $\pi^2/3$ describing $\langle \phi^2 \rangle$ for small forces to a power law $k_B T / f\ell_p$ for $f\ell_p/k_B T > 1$, as in $d = 2$ dimensions, the behavior of the fluctuations in the chain linear dimensions clearly is rather complicated. Of course, there is a

need to extend the scaling analysis, that was presented for $\langle X \rangle$ as a function of $f\ell_p/k_B T$ in Fig. 1(b) to the fluctuations $\langle X^2 \rangle - \langle X \rangle^2$ and $\langle R_{\perp}^2 \rangle$ in greater detail than we have done so far. We expect that analyzing these fluctuations should yield additional and valuable information on the structure of stretched semiflexible chains, and allow to pin down the parameters needed to relate experimental data to theoretical models more precisely. We plan to tackle this task in a forthcoming study.

VII. CONCLUSION

In this paper, we have studied self-avoiding walks on square and simple cubic lattices, where an energy penalty ϵ_b associated with chain bending to model semiflexibility of the polymer chains, by extensive Monte Carlo simulations, using the PERM algorithm. We have obtained both force versus extension curves and chain linear dimensions in the absence of forces for a wide range of chain lengths N_b (typically N_b up to 25600) and chain stiff-

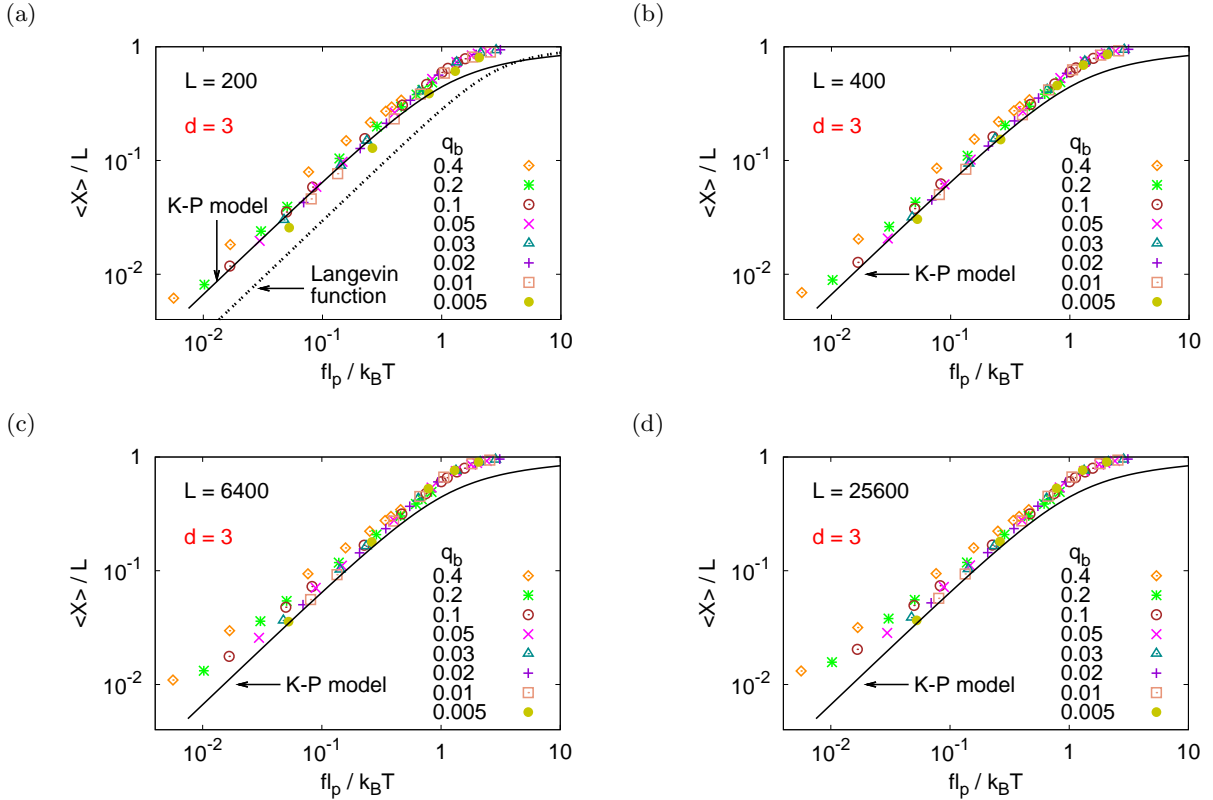


FIG. 14: Log-log plot of $\langle X \rangle / L$ versus $f \ell_p / k_B T$ for several choices of q_b as indicated, for contour length $L = 200$ (a), $L = 400$ (b), $L = 6400$ (c), and $L = 25600$ (d). Full curve always refers to the K-P model prediction, Eq. (54). Broken curve in (a) is the Langevin function, Eq. (4), using $\ell_p / \ell_b = 0.71$ for $q_b = 0.4$ (Table II). Data are for semiflexible chains in $d = 3$.

ness (characterized by $q_b = \exp(-\epsilon_b / k_B T)$). In Sec. II, we have attempted to present a coherent phenomenological theoretical description, combining results from scaling concepts with other results derived from the Kratky-Porod model, to explain the various crossovers that can occur in the force versus extension curves for various circumstances (Fig. 1). We have emphasized that the case of $d = 2$ dimensions is rather different from the case $d = 3$: only in the latter case one can identify a linear regime in the force versus extension curve that is compatible with the Kratky-Porod model; the linear response regime both in $d = 2$ and $d = 3$ dimensions is strongly affected by the presence of excluded volume effects, and for long enough chains is followed by a nonlinear (“Pincus blob”) regime for stronger forces both in $d = 2$ and $d = 3$ dimensions. However, for very stiff and not too long chains in $d = 3$ the chains in the absence of a force show Gaussian behavior, and in this case the stretched chains do not exhibit the nonlinear Pincus blob regime, and the Kratky-Porod model holds throughout (apart from very strong forces, where the discrete character of polymer chains matter).

The Monte Carlo data that we have generated do provide evidence for these concepts, particularly in the relatively simple case of $d = 2$ dimensions. While in $d = 2$ all expected regimes of the force vs. extension curves are

confirmed and the expected scaling behavior is verified, problems remain concerning the precise understanding of longitudinal and transverse fluctuations of chain linear dimensions of the chains. More work on these aspects (from theory, simulation, and experiment) clearly is desirable. We recall that imaging techniques can provide rather detailed information on chain configurations of semiflexible polymers adsorbed on substrates; we expect that our work should be useful to interpret such experiments.

In the case of $d = 3$ dimensions, our numerical evidence is much more limited: chain lengths $N_b = 25600$ clearly do not suffice to fully resolve three distinct power laws (separated by smooth crossovers) in the force versus extension curves. However, simulations for chains that are one or two orders of magnitude larger clearly are not feasible at present. We do obtain evidence, however, that for rather stiff thin short chains excluded volume effects indeed are negligible, as expected, and hence the Kratky-Porod model holds. However, when chain stiffness is due to thickness (persistence length ℓ_p being proportional to local chain diameter D), the regime of Gaussian statistics disappears and rather excluded volume effects dominate throughout, resulting in a rather broad regime where the force versus extension curve is nonlinear already for small

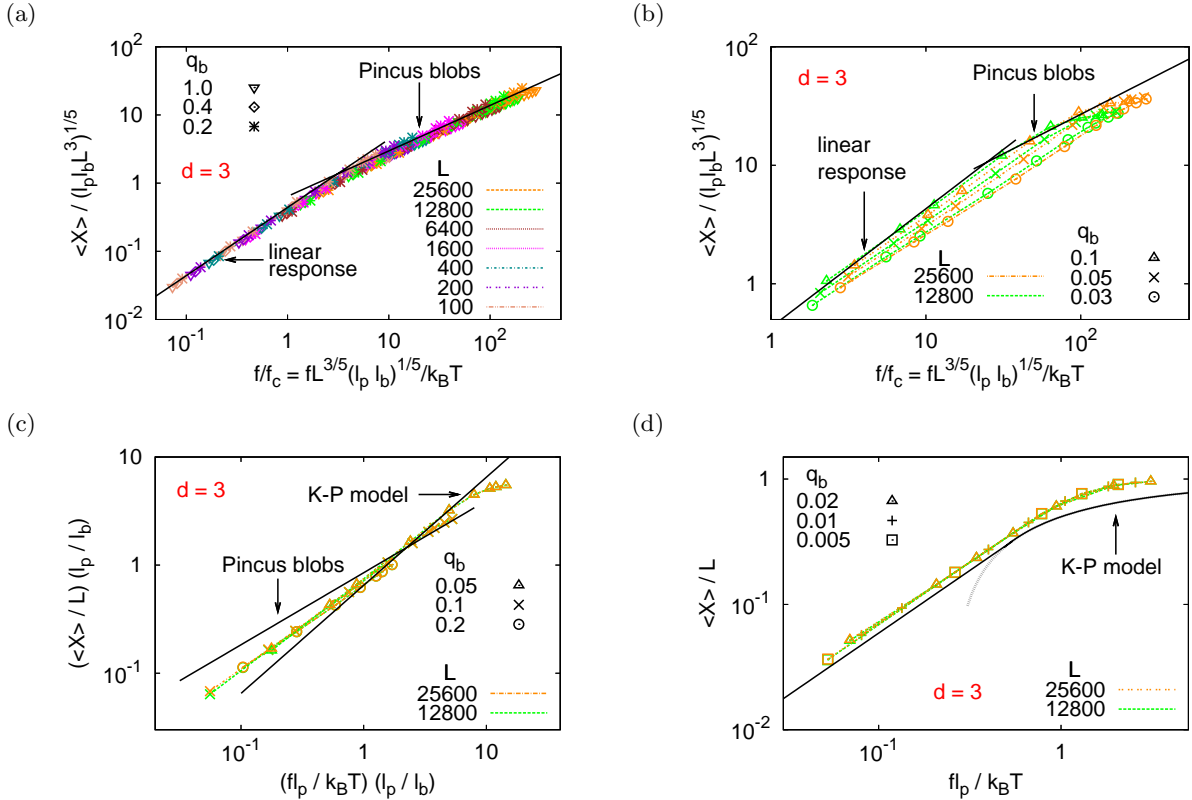


FIG. 15: (a) Log-log plot of $\langle X \rangle / (\ell_p \ell_b L^3)^{1/5}$ vs $f/f_c = f L^{3/5} (\ell_p \ell_b)^{1/5} / k_B T$, where f_c is the crossover force defined in Eq. (60), remembering $D = \ell_b$ in our model, for the choices $q_b = 1.0, 0.4$, and 0.2 and many choices of L (a) and for $q_b = 0.1, 0.05, 0.03$ but only $L = 25600$ and $L = 12800$ (b). Case (c) shows a plot of $(\langle X \rangle / L) (\ell_p / \ell_b)$ versus $(f \ell_p / k_B T) (\ell_p / \ell_b)$ for the choices $q_b = 0.05, 0.1$, and 0.2 , again for $L = 25600$ and $L = 12800$ only, to test for indications of a crossover from Pincus blobs to the Kratky-Porod model, showing only the vicinity of the region when this crossover should occur. Case (d) is a blow up the region $0.05 \leq \langle X \rangle / L < 0.5$, for $q_b = 0.02, 0.01, 0.05$, $L = 25600$ and $L = 12800$, to show the full K-P region for rather long and rather stiff chains. Data are for semiflexible chains in $d = 3$.

$\langle X \rangle / L$. Also for rather flexible chains, clear evidence for the Pincus blob regime is obtained (Fig. 15(a)).

In our modelling, we have approximated the interactions between monomers of the chain as a strictly local excluded volume interaction. Of course, in many cases of interest the interactions are of longer range, e.g. because of electrostatic interactions between charged groups. Particularly for polyelectrolytes the resulting problem of an “electrostatic persistence length” has received longstanding attention in the literature [56, 77–79]. Molecules such as DNA and RNA do possess a substantial linear charge density, and the properties of such polyelectrolytes, in fact, will depend on the electrostatic screening due to ions in the solution, and thus the effective persistence length will depend on ionic strength. In this context, the concept of an “effective thickness” of polyelectrolytes, that are described in terms of a “thick chain model” [79], has been used to model experimental extension versus force curves. It will be an interesting task for the future, beyond the scope of the present paper, to clarify the extent to which such approaches are

equivalent to the scaling concepts applied here. In any case, it is very reassuring that very recently, after our study was completed, single-molecule elasticity measurements of the onset of excluded volume effects of stretched poly(ethylene glycol) were published [80]. In this work, the Pincus blob scaling behavior ($L \propto f^{2/3}$ in $d = 3$ dimensions) could be seen under several circumstances, followed by a crossover to the linear behavior ($L \propto f$) and subsequent saturation, compatible with the behavior predicted by the K-P model. The interpretation given in Ref. [80] for these experiments is fully consistent with the description given in the present paper. Some earlier evidence for the Pincus behavior was also found for DNA [81, 82].

In our simulations, we have not considered the effects of varying the diameter D of our chains (we have chosen $D = \ell_b = 1$, the lattice spacing, throughout). For biopolymers D is a parameter of great interest as well [82], of course. In our studies of bottlebrush polymers [43, 44], however, we studied conditions for which $D \propto \ell_p$, and then the K-P model was not useful even in

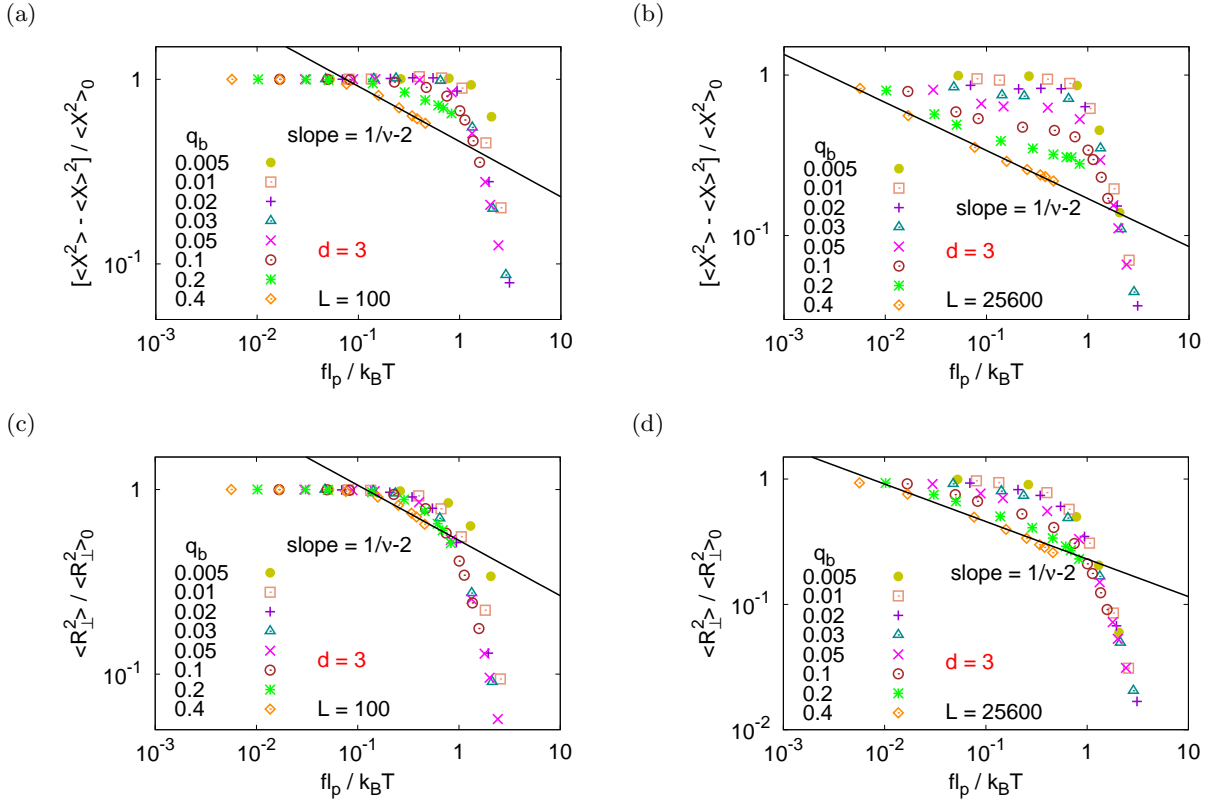


FIG. 16: Log-log plot of $[\langle X^2 \rangle - \langle X \rangle^2] / \langle X^2 \rangle_0$ vs. $f l_p / k_B T$ for $L = 100$ (a) and $L = 25600$ (b), and for various choices of q_b , as indicated. Part (c) shows analogous data for $\langle R_{\perp}^2 \rangle / \langle R^2 \rangle_0$ vs. $f l_p / k_B T$ for $L = 100$ and part (d) for $L = 25600$. A straight line with slope $1/\nu - 2$ ($\nu = 0.588$) is shown for comparison. Data are for semiflexible chains in $d = 3$.

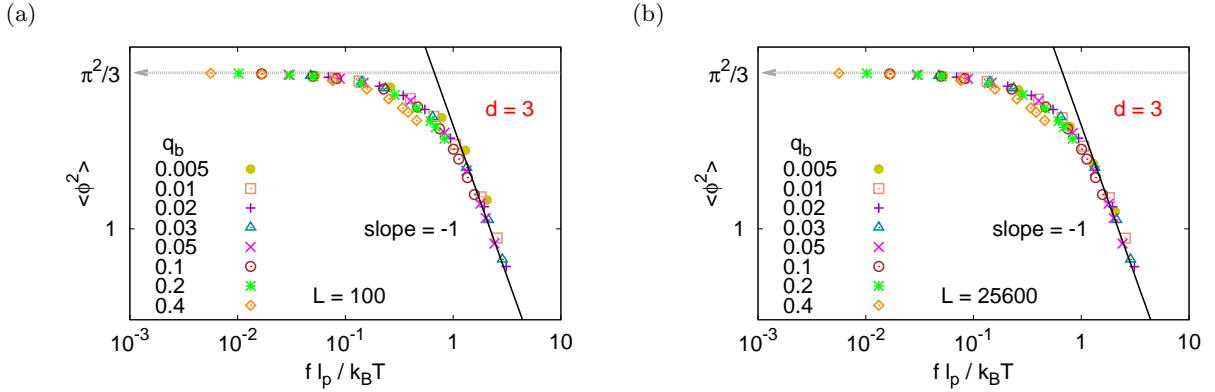


FIG. 17: Log-log plot of $\langle \phi^2 \rangle$ vs. $f l_p / k_B T$ for $L = 100$ (a) and $L = 25600$ (b), and for many choices of q_b , as indicated. $\langle \phi^2 \rangle = \pi^2/3$ as $f \rightarrow \infty$. Data are for semiflexible chains in $d = 3$.

$d = 3$ dimensions.

Thus we hope that the present work will contribute to the better understanding of both existing and future experiments. A very interesting aspect, completely beyond the scope of the present work, are dynamic properties of stretched semiflexible polymers in solution, see e.g. Ref. [83]. Our study should yield useful inputs for such

problems, too.

Acknowledgments

This work have been supposed by the Deutsche Forschungsgemeinschaft (DFG) under grant No SFB

625/A3. We are particularly grateful to Wolfgang Paul for his fruitful collaboration on some early aspects of this work. Stimulating discussions with Ralf Everaers, Carlo

Pierleoni, and Hyuk Yu are acknowledged. We thank the NIC Jülich for a generous grant of computer time on the JUROPA supercomputer.

-
- [1] P. J. Flory, *Statistical Mechanics of Chain Molecules* (Wiley, New York, 1969).
- [2] M. V. Volkenshtein and O. B. Ptitsyn, *Sov. Phys. JETP* **25**, 649 (1955).
- [3] M. Fixman and J. Kovac, *J. Chem. Phys.* **58**, 1564 (1973).
- [4] R. G. Treloar, *Physics of Rubber Elasticity*, 3rd ed. (Clarendon Press, Oxford, 1975).
- [5] P. Pincus, *Macromolecules* **9**, 386 (1976).
- [6] P. G. de Gennes, *Scaling Concepts in Polymer Physics* (Cornell Univ. Press, Ithaca, N. Y., 1979).
- [7] I. Webman, J. L. Lebowitz, and M. H. Kalos, *Phys. Rev. A* **23**, 316 (1981).
- [8] J. Kovac and C. C. Crabb, *Macromolecules* **15**, 537 (1982).
- [9] A. Yu. Grosberg and A. R. Khokhlov, *Statistical Physics of Macromolecules* (AIP Press, N. Y., 1994).
- [10] M. Wittkop, J.-U. Sommer, S. Kreitmeier and D. Göritz, *Phys. Rev. E* **49**, 5472 (1994).
- [11] P. Cifra and T. Blaha, *J. Chem. Soc. Faraday Trans.* **91**, 2465 (1995).
- [12] J. F. Marko and E. D. Siggia, *Macromolecules* **28**, 8759 (1995).
- [13] K. Kroy and E. Frey, *Phys. Rev. Lett.* **77**, 306 (1996).
- [14] C. Pierleoni, G. Ariedi and J.-P. Ryckaert, *Phys. Rev. Lett.* **79**, 2990 (1997).
- [15] D. Bensimon, D. Dohmi, and M. Mézard, *Europhys. Lett.* **42**, 97 (1998).
- [16] J. J. Titantah, C. Pierleoni, and J.-P. Ryckaert, *Phys. Rev. E* **60**, 7010 (1999).
- [17] A. Lamura, T. W. Burkhardt, and G. Gompper, *Phys. Rev. E* **64**, 061801 (2001).
- [18] R. R. Netz, *Macromolecules* **34**, 7522 (2001).
- [19] L. Livadaru, R. R. Netz, and H. J. Kreuzer, *Macromolecules* **36**, 3732 (2003).
- [20] R. G. Winkler, *J. Chem. Phys.* **118**, 2919 (2003).
- [21] A. Rosa, T. X. Hoang, D. Marenduzzo, and A. Maritan, *Macromolecules* **36**, 10095 (2003).
- [22] J. Kierfeld, O. Niamploy, V. Sa-yakanit, and R. Lipowsky, *Eur. Phys. J. E* **14**, 17 (2004).
- [23] T. Hugel, M. Rief, M. Seitz, H. E. Gaub, and R. R. Netz, *Phys. Rev. Lett.* **94**, 048301 (2005).
- [24] A. Prasad, Y. Hori, and J. Kondev, *Phys. Rev. E* **72**, 041918 (2005).
- [25] G. Morrison, C. Hyeon, N. M. Toan, B.-Y. Ha, and D. Thirumalai, *Macromolecules* **40**, 7343 (2007).
- [26] J. Krawczyk, I. Jensen, A. L. Owczarek, and S. Kumar, *Phys. Rev. E* **79**, 031912 (2009).
- [27] A. V. Dobrynin, J.-M. Y. Carrillo, and M. Rubinstein, *Macromolecules* **43**, 9181 (2010).
- [28] N. M. Toan and D. Thirumalai, *Macromolecules* **43**, 4394 (2010).
- [29] S. Kumar and M. S. Li, *Phys. Rep.* **486**, 1 (2010).
- [30] S. B. Smith, L. Finzi, and C. Bustamante, *Science* **258**, 1112 (1992); M.-N. Dessinges, B. Maier, Y. Zhang, M. Peliti, D. Bensimon, and V. Croquette, *Phys. Rev. Lett.* **89**, 248102 (2002); Y. Seol, G. M. Skinner, and K. Visscher, *Phys. Rev. Lett.* **93**, 118102 (2004).
- [31] J. Liphardt, B. Onoa, S. B. Smith, I. Tinoco Jr. and C. Bustamante, *Science* **292**, 733 (2001).
- [32] M. Grandbois, M. Beyer, M. Rief, H. Clausen-Schaumann and H. E. Gaub, *Science* **283**, 1727 (1999).
- [33] M. Rief, M. Gautel, F. Oesterhelt, J. M. Fernandez and H. E. Gaub, *Science* **276**, 1109 (1997).
- [34] N. Gunari, M. Schmidt, and A. Janshoff, *Macromolecules* **39**, 2219 (2006).
- [35] A. Halperin and E. B. Zhulina, *Europhys. Lett.* **15**, 417 (1991).
- [36] D. Marenduzzo, A. Maritan, A. Rosa, and F. Seno, *Eur. Phys. J. E* **15**, 83 (2004).
- [37] D. Marenduzzo, A. Maritan, A. Rosa, and F. Seno, *Phys. Rev. Lett.* **90**, 088301 (2003).
- [38] S. Kumar and G. Mishra, *Phys. Rev. E* **78**, 011907 (2008).
- [39] S. Stepanow, *Eur. Phys. J. B* **39**, 499 (2004).
- [40] A. A. Gorbunov and A. M. Skvortsov, *J. Chem. Phys.* **98**, 5961 (1993).
- [41] S. Bhattacharya, V. G. Rostiashvili, A. Milchev, and T. A. Vilgis, *Macromolecules* **42**, 2236 (2009).
- [42] A. M. Skvortsov, L. I. Klushin, G. J. Fleer, and F. A. Leermakers, *J. Chem. Phys.* **132**, 064110 (2010).
- [43] H.-P. Hsu, W. Paul, and K. Binder, *Macromolecules* **43**, 3094 (2010).
- [44] H.-P. Hsu, W. Paul, and K. Binder, *EPL* **92**, 28003 (2010); *Macromol. Theory & Simul.* **20**, 510 (2011).
- [45] H.-P. Hsu, W. Paul, and K. Binder, *EPL* **95**, 68004 (2011).
- [46] L. Schäfer, A. Ostendorf, and J. Hager, *J. Phys.* **A32**, 7875 (1999).
- [47] O. Kratky and G. Porod, *J. Colloid Sci.* **4**, 35 (1949).
- [48] N. Saito, K. Takahashi, and Y. Yunoki, *J. Phys. Soc. Japan* **22**, 219 (1967).
- [49] L. Schäfer and K. Elsner, *Eur. Phys. J. E* **13**, 225 (2004).
- [50] R. Everaers, A. Milchev and V. Yamakov, *Eur. Phys. J. E* **8**, 3 (2002).
- [51] M. Rubinstein and R. H. Colby, *Polymer Physics* (Oxford Univ. Press, Oxford, 2003).
- [52] J. C. LeGuillou and J. Zinn-Justin, *Phys. Rev. B* **21**, 3976 (1980).
- [53] J. Des Cloizeaux and G. Jannink, *Polymers in Solution: Their Modelling and Structure* (Clarendon Press, Oxford, 1990).
- [54] P.-M. Lam, *Biopolymers* **64**, 57 (2002).
- [55] S. F. Edwards and P. Singh, *J. Chem. Soc., Faraday Trans.* **2**, 75, 1001 (1979).
- [56] R. G. Winkler, P. Reineker and L. Harnau, *J. Chem. Phys.* **101**, 8119 (1994).
- [57] K. Kremer and K. Binder, *Computer Phys. Rep.* **7**, 259 (1988).
- [58] D. W. Schaefer, J. F. Joanny, and P. Pincus, *Macromolecules* **13**, 1280 (1980).
- [59] R. R. Netz and D. Andelman, *Phys. Rep.* **380**, 1 (2003).

- [60] T. Norisuye and H. Fujita, *Polymer J.* **14**, 143 (1982).
- [61] T. Odijk, *Macromolecules* **16**, 1340 (1983).
- [62] T. Odijk, *Macromolecules* **17**, 502 (1984).
- [63] J. Wilhelm and E. Frey, *Phys. Rev. Lett.* **77**, 2581 (1996).
- [64] D. Thirumalai and B.-Y. Ha, cond-mat/9705200
- [65] J. K. Bhattacharjee, D. Thirumalai, and J. D. Bryngelson, cond-mat/9709345.
- [66] J. Samuel and S. Sinha, *Phys. Rev. E* **66**, 050801 (2002).
- [67] A. Dhar and D. Chaudhuri, *Phys. Rev. Lett.* **89**, 065502 (2002).
- [68] C. R. Cantor and P. R. Schimmel, *Biophysical Chemistry, Part III, The Behavior of Biological Macromolecules* (W. H. Freeman, San Francisco, 1980).
- [69] R. Lavery, A. Lebrun, J.-F. Allemand, D. Bensimon and V. Croquette, *J. Phys.: Condens. Matter* **14**, R383 (2002).
- [70] P. Virnau, Y. Kantor, and M. Kardar, *J. Am. Chem. Soc.* **127**, 15102 (2005).
- [71] A. Borgia, P. M. Williams, and J. Clarke, *Annu. Rev. Biochem.* **77**, 101 (2008).
- [72] P. Virnau, A. Mallam, and S. Jackson, *J. Phys.: Condens. Matter* **23**, 033101 (2011).
- [73] P. Grassberger, *Phys. Rev. E* **56**, 3682 (1997).
- [74] U. Bastolla and P. Grassberger, *J. Stat. Phys.* **89**, 1061 (1997).
- [75] H.-P. Hsu and P. Grassberger, *J. Stat. Phys.* **144**, 597 (2011).
- [76] N. Yoshinaga, K. Yoshikawa, and S. Kidoaki, *J. Chem. Phys.* **116**, 9926 (2002).
- [77] U. Micka and K. Kremer, *Phys. Rev. E* **54**, 2653 (1996).
- [78] M. Ullner, B. Jönsson, C. Peterson, O. Sommelius, and B. Söderberg, *J. Chem. Phys.* **107**, 1279 (1997); M. Ullner, and C. E. Woodward, *Macromolecules* **35**, 1437 (2002).
- [79] N. M. Toan and C. Micheletti, *J. Phys.: Condens. Matter* **18**, S269 (2006).
- [80] A. Dittmore, D. B. McIntosh, S. Halliday, and O. A. Saleh, *Phys. Rev. Lett.* **107**, 148301 (2011).
- [81] O. A. Saleh, D. B. McIntosh, P. Pincus, and N. Ribeck, *Phys. Rev. Lett.* **102**, 068301 (2009); D. B. McIntosh, N. Ribeck, and O. A. Saleh, *Phys. Rev. E* **80**, 041803 (2009).
- [82] N. M. Toan, D. Marenduzzo, and C. Micheletti, *Biophys. J.* **89**, 80 (2005).
- [83] J. W. Hatfield and S. R. Quake, *Phys. Rev. Lett.* **82**, 3548 (1999).

